CLIMATE VARIABILITY AND PREDICTION

Climate variability and prediction is a central scientific theme within NASA's Earth Science Program. To understand climate variability, an integrated program of observations and modeling of air-sea-ice interactions and their feedbacks are required. The following professional papers for the year 2002 by the NASA researchers have spanned the entire globe with special focus on the poles as harbingers of climate change.

The Greenland and Antarctic ice sheets with their massive ice sheets are of especial interest for climate change and societal impact. Bindschadler and Bentley note that the West Antarctic ice sheet contains more than three million cubic kilometers of fresh water. Previously it had been thought that this ice sheet was in a stage of rapid collapse which could raise global sea level five meters with major societal effect. However, it now appears that the ice sheet is shrinking more slowly than originally suspected and thus a sea level rise of half a meter during the next century is more likely, still a fact for planners to anticipate. Obviously temperature in the Antarctic region will be crucial for prediction of ice melt. Shuman and Comiso have studied data from in situ weather stations with AVRR and SSM/I satellite data to determine how best to use NASA satellite to observe regional small temperature changes. This study has enabled an improved understanding of the three available data sets. At present, the thermal infrared data provide the only spatially detailed temperature distributions in Antarctica, but contain data gaps due to intermittent cloud cover. The passive-microwave data have the potential to provide spatially detailed, continuous and gap-free temperature distributions; however calibrations with weather station data requires more work.

Sea ice is an indicator of global change as its extent and volume reflect temperature changes in both the surface and water column. Zwally et al. analyzed passive microwave observations to study the variability of Antarctic sea ice from 1979 to 1998. They show that in recent decades the sea ice cover has varied significantly from year to year with some anomalies persisting for periods of 3-5 years. Over the 20 year study period, the entire sea ice pack increased about 11,180 km2. The largest increase was in the autumn ice cover, but there was significant regional variability. Parkinson in a related study analyzed the length of the southern sea ice season for the same time period showing an overall lengthening of the sea ice season with significant spatial variability. Specifically, most of the Ross Sea ice cover has undergone a lengthening of the season; whereas most of the Amundson Sea ice cover and almost all the Bellinghausen Sea ice cover has undergone a shortening of the sea ice season, and the Weddell Sea is mixed. Two papers by Kwok and Comiso analyzed the spatial patterns of temperature over both the Antarctic continent and the adjacent ocean. Their data revealed a 17-year (1982-1998) cooling over the continent and a warming of the sea-ice zone, but moderate changes over the oceans. As expected the warming of the seas is in regions where sea ice is shrinking as noted by Parkinson. Kwok and Comiso relate the effects of the Southern Hemisphere Annular Mode (SAM) and the extra-polar Southern Oscillation (SO) on surface temperature through regression analysis. Positive polarities of the SAM are associated with cold anomalies over most of Antarctic, with the most notable exception of the Antarctic Peninsula. Positive temperature anomalies and the ice edge retreat in the Pacific sector are shown to be associated with El-Nino episodes.

The Arctic Ocean is the smallest of the Earth's oceans and unlike Antarctica is surrounded by land-masses. Its temperature, salinity and ice cover have all undergone changes in the past several decades. As Parkinson notes it is uncertain whether these reflect long-term changes or oscillations within the system. Parkinson and Cavalieri have documented 2.7 km2 per decade reduction in sea ice extent from satellite passive-microwave data (1979-1999). These negative trends are statistically significant at a 99% confidence level. Comiso in two papers made use of simultaneous satellite sea-ice concentration and surface data to gain insight into the changing Arctic climate. In general sea ice extent has been declining at a rate 2.3% per decade while surface temperature has increased by 0.4 K per decade. If this continues, it means that the multi-year sea ice will disappear during this century.

To extract significant information from varied climate data, Vinnikov et al have developed a new statistical approach to analyze climatic data that explicitly accepts the idea that long-term climatic records contain trends in means, variances, covariances and other moments of statistical distribution of meteorological variables. This approach will provide better analysis of past climate change and climatic model output of existing data.

Another statistical approach was presented by Chen et al. to address the feasibility of using collocated wind speed and significant wave height measurements from simultaneous scatterometer and altimeter to observe the spatial and seasonal pattern of dominant swell and wind waves in the world's oceans. Knowledge of these parameters on a global basis is generally poor. Based on this method they found swell dominance in the eastern tropical areas of the Pacific, the Atlantic and Indian Oceans; wave growth areas are the northwest Pacific, Atlantic, the Southern Ocean and Mediterranean.

On a more local scale and closer to GSFC, Foster describes the recent spate of tornados in Maryland in comparison to previous occurrences of extreme weather events. These are attributed to an energetic cold front acting as a triggering mechanism for tornado formation when a large area of moisture is surging north from the Gulf of Mexico and a vigorous jet stream is positioned overhead.

On Thin Ice?

BY ROBERT A. BINDSCHADLER AND CHARLES R. BENTLEY

Twelve thousand years ago, as the earth emerged from the last ice age,

vast armadas of *Titanic*-size icebergs invaded the North Atlantic. Purged vigorously from the enormous ice sheets that smothered half of North America and Europe at the time, those icebergs displaced enough water to raise global sea level more than a meter a year for decades.

As the frozen north melted, the ice gripping the planet's southernmost continent remained essentially intact and now represents 90 percent of the earth's solid water. But dozens of scientific studies conducted over the past 30 years have warned that the ice blanketing West Antarctica—the part lying mainly in the Western Hemisphere—could repeat the dramatic acts of its northern cousins. Holding more than three million cubic kilometers of freshwater in its frozen clutches, this ice sheet would raise global sea level five meters (about 16 feet) if it were to disintegrate completely, swamping myriad coastal lowlands and forcing many of their two billion inhabitants to retreat inland.

Most Antarctic scientists have long concurred that the continent's ice has shrunk in the past, contributing to a rise in sea level that continued even after the northern ice sheets were gone. The experts also agree that the ice covering the eastern side of the continent is remarkably stable relative to that in West Antarctica, where critical differences in the underlying terrain make it inherently more erratic. But until quite recently, they disagreed over the likelihood of a catastrophic breakup of the western ice sheet in the near future. Many, including one of us (Bindschadler), worried that streams of ice flowing from the continent's interior toward the Ross Sea might undermine the sheet's integrity, leading to its total collapse in a few centuries or less. Others (including Bentley) pointed to the sheet's recent persistence, concluding that the sheet is reasonably stable.

For a time it seemed the debate might never be resolved. Agreement was hampered by scant data and the challenge of studying a continent shrouded half the year in frigid darkness. In addition, although areas of the ice sheet have drained quickly in the past, it is difficult to determine whether changes in the size or speed of the ice seen today are a reflection of normal variability or the start of a dangerous trend. In the past few years, though, a variety of field and laboratory studies have yielded a growing consensus on the forces controlling West Antarctica's future, leading experts in both camps to conclude that the ice streams pointing toward the Ross Sea are not currently as threatening as some of us had feared.

We remain puzzled, however, over the ice sheet's ultimate fate. New studies have revealed thinning ice in a long-neglected sector of West Antarctica, suggesting that a destructive process other than ice streams is operating there. And another region—the peninsula that forms Antarctica's northernmost arm—has recently experienced warmer summer temperatures that are almost certainly the reason behind an ongoing breakup of ice along its coasts.

Around the world temperatures have risen gradually since the end of the last ice age, but the trend has accelerated markedly since the mid-1990s with the increase of heat-trapping greenhouse gases in the atmosphere. So far the peninsula seems to be the only part of Antarctica where this recent climate trend has left its mark; average temperatures elsewhere have risen less or even cooled slightly in the past 50 years. Researchers are now scrambling to determine whether global warming is poised to gain a broader foothold at the bottom of the world.

Overview/*Antarctic Ice*

- For nearly three decades, numerous Antarctic experts warned that West Antarctica's ice sheet is in the midst of a rapid disintegration that could raise global sea level five meters in a few centuries or less.
- Many of those researchers now think that the ice sheet is shrinking much more slowly than they originally suspected and that sea level is more likely to rise half a meter or less in the next century.
- That consensus is not without its caveats. The ice sheet's poorly understood Amundsen sector now appears to be shrinking faster than previously thought.
- Global warming, which has so far played a negligible role in West Antarctica's fate, is bound to wield greater influence in the future.

Early Alarms

INDICATIONS THAT the West Antarctic ice sheet might be in the midst of a vanishing act first began cropping up about 30 years ago. In 1974 Johannes Weert-

PAST, PRESENT AND FUTURE?

ANTARCTICA'S THICK BLANKET OF ICE (*below*) has been contracting, mostly gradually but sometimes swiftly, since the height of the last ice age, 20,000 years ago. The greatest reduction has occurred in West Antarctica, where the ice sheet is considerably more fragile than its counterpart in the east. Because the western sheet has changed quickly in the past, scientists have been unsure whether recent dramatic ice losses reflect normal variability or the start of an ominous trend toward total collapse. In the wake of a catastrophic collapse, rapidly rising seas would flood coastal communities around the world. *—R.A.B. and C.R.B.*

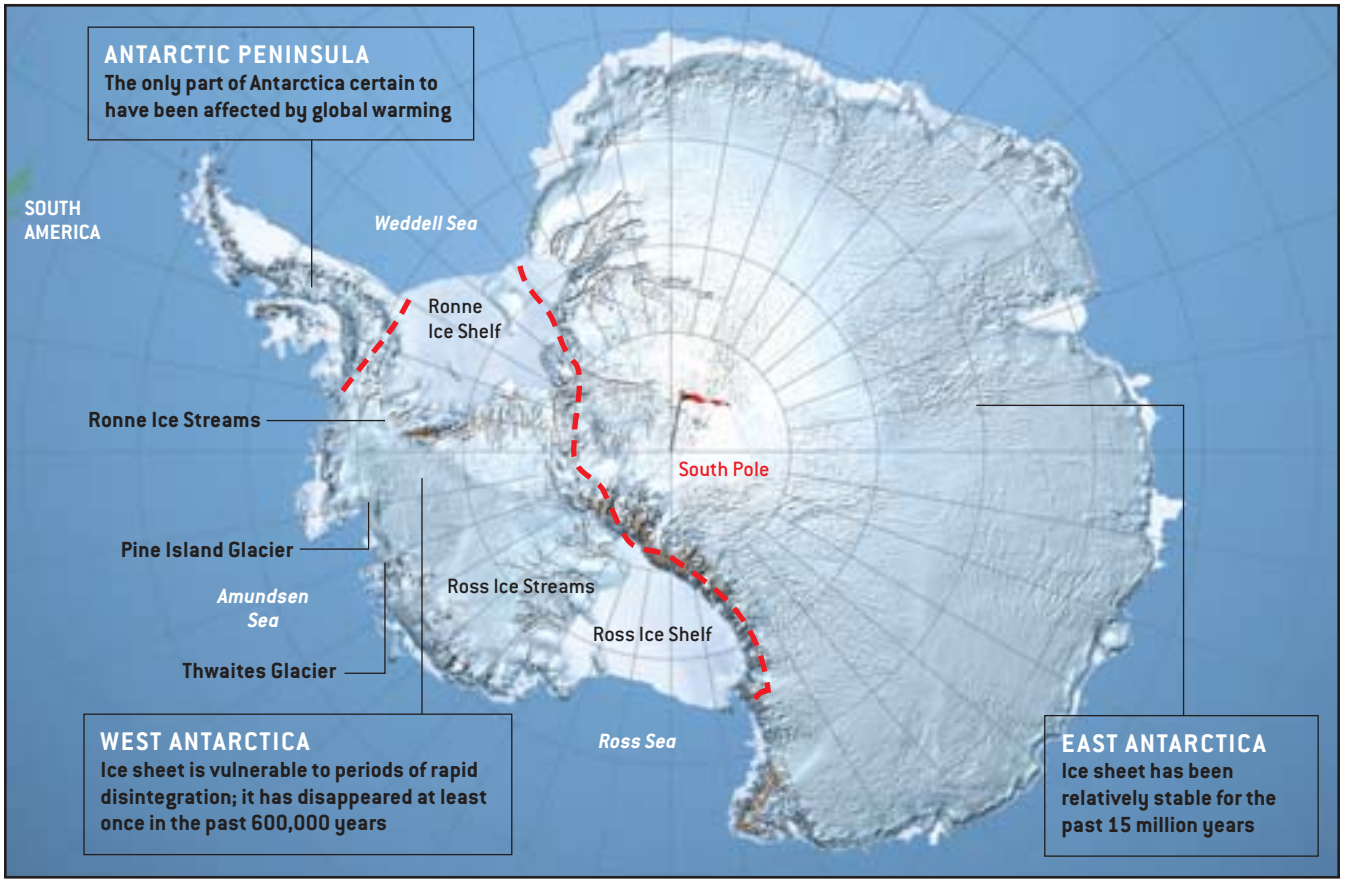

SHEDDING AND SHRINKING

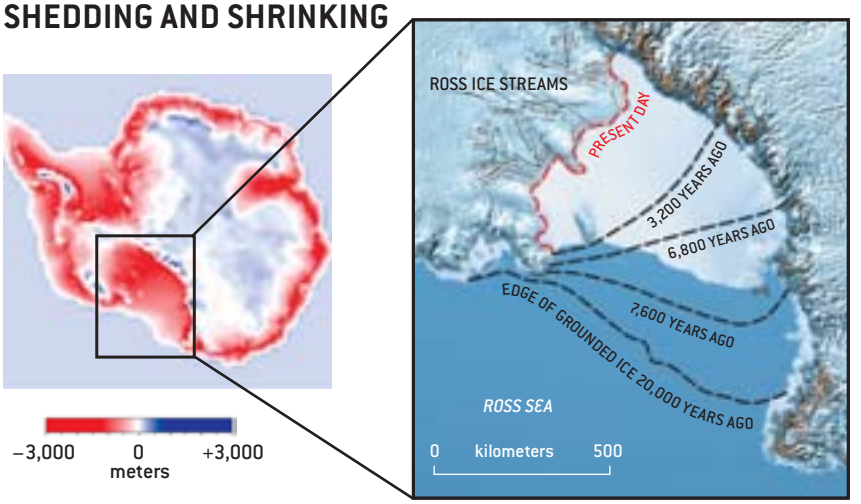

CHANGE IN ICE THICKNESS since the last ice age (*above left*) translates into a loss (*red*) of about 5.3 million cubic kilometers, much of it from West Antarctica. The ice sheet's grounded edge, that reaching the seafloor, has shrunk particularly rapidly in the Ross Sea (*detail, right*) over the past 7,000 years, retreating some 700 kilometers inland.

THE WORST-CASE SCENARIO

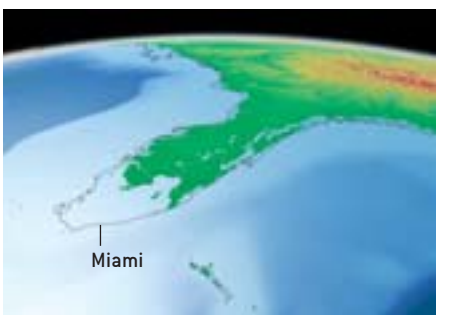

COMPLETE COLLAPSE of West Antarctica's ice sheet would raise sea level five meters. Among the casualties would be southern Florida (*above*), where about a third of the famous peninsula would disappear underwater. Today West Antarctica contributes about 10 percent of the average sea-level rise of two millimeters a year.

DAVID FIERSTEIN (*main Antarctica map and Ross Ice Shelf map*); ROBERT A. BINDSCHADLER (*ice thickness map*); WILLIAM F. HAXBY (*Florida map*)

A Global View of Swell and Wind Sea Climate in the Ocean by Satellite Altimeter and Scatterometer

GE CHEN

Ocean Remote Sensing Institute, Ocean University of Qingdao, Qingdao, China

BERTRAND CHAPRON AND ROBERT EZRATY

Département d'Océanographie Spatiale, Centre de Brest, IFREMER, Plouzane, France

DOUGLAS VANDEMARK

Wallops Flight Facility, NASA Goddard Space Flight Center, Wallops Island, Virginia

(Manuscript received 8 August 2001, in final form 18 February 2002)

ABSTRACT

Numerous case reports and regional studies on swell and wind sea events have been documented during the past century. The global picture of these common oceanic phenomena, however, is still incomplete in many aspects. This paper presents a feasibility study of using collocated wind speed and significant wave height measurements from simultaneous satellite scatterometer and altimeter sources to observe the spatial and seasonal pattern of dominant swell and wind wave zones in the world's oceans. Two energy-related normalized indices are proposed, on the basis of which global statistics of swell/wind sea probabilities and intensities are obtained. It is found that three well-defined tongue-shaped zones of swell dominance, termed ''swell pools,'' are located in the eastern tropical areas of the Pacific, the Atlantic, and the Indian Oceans, respectively. Regions of intensive wave growth are observed in the northwest Pacific, the northwest Atlantic, the Southern Ocean, and the Mediterranean Sea. Seasonality is distinct for the climate of both swell and wind sea, notably the large-scale northward bending of the swell pools in boreal summer, and the dramatic shift of wave-growing extent from a summer low to an autumn high. The results of this study may serve as a useful reference for a variety of activities, such as ocean wave modeling, satellite algorithm validation, coastal engineering, and ship routing, when information on swell and wind sea conditions is needed.

1. Introduction

Waves are one of the most fundamental and ubiquitous phenomena present at the air–sea interface. Since the spectrum of ocean waves is continuous and infinite, they are likely to cover a wide range of frequency and wavelength. The dominant portion of the wave spectrum in terms of energy is known to be associated with gravity waves whose period ranges from 1 to 30 s [see, e.g., Figs. 1.2–1 of Kinsman (1965)]. Therefore it comes as no surprise that a majority of ocean wave studies are devoted to gravity waves.

Two main classes of gravity waves exist in the ocean, namely, the so-called wind wave (or wind sea when emphasizing its state) and swell. The former refers to young waves under growth or in equilibrium with local wind, while the latter is defined as waves generated elsewhere and propagating over large distances. As a rule of thumb, a period of 10 s may be taken as separating swell from wind wave (Kinsman 1965). Because of the different dynamics involved, studies on swell and wind wave usually have different motivations and concerns. Swell is of increasing concern because of its potentially destructive consequences on coastal structures and sea-going activities (Mettlach et al. 1994). For example, in October 1987 nine elementary school children were drowned by the sudden arrival of a typhoon-generated swell hitting the Mau-Pi-Tou coast of Taiwan (Liang 1990). On the other hand, wind wave with a fetch up to an equilibrium state is of particular importance for the development and verification of wave models. Many previous studies, both theoretical and experimental, have been carried out in this regard (e.g., Pierson and Moskowitz 1964; Hasselmann et al. 1973; Hasselmann et al. 1988; Kahma 1981; Ewing and Laing 1987; Ebuchi et al. 1992).

In view of the different natures and impacts of swell and wind sea, a global knowledge of each individual process in terms of its frequency of occurrence and associated energy is highly desirable. This can be quickly understood by examining the prerequisites of the two categories of studies outlined above. Analysis of swell energy and prediction of its propagation would obviously benefit from a zero-wind condition. On the other hand, a wind-wave-related investigation always seeks an ideal sea state with no swell presence, especially when time and site have to be determined or selected for a field experiment. Despite their different dynamics,

Corresponding author address: Dr. Ge Chen, Ocean Remote Sensing Institute, Ocean University of Qingdao, 5 Yushan Road, Qingdao 266003, China.
E-mail: gechen@public.qd.sd.cn

swell and wind sea often overlap in wave characteristics. Moreover, they are usually a complex mixture at a given location. This sometimes makes it difficult to separate the two phenomena in real observations. In this study, taking the advantage of the newly available simultaneous measurements from National Aeronautics and Space Administration (NASA) satellite sensors, the TOPEX altimeter and the NSCAT and QuikSCAT (hereinafter abbreviated as QSCAT) scatterometers, an energy-based scheme is proposed to estimate the respective degree of swell and wind wave for each collocation site (section 2), on the basis of which global maps of swell and wind sea climate are produced and analyzed (sections 3 and 4). Finally, major swell and wind wave zones in the world's oceans are discussed and summarized (section 5).

2. Data and scheme

a. Wind–wave relation

According to wave forecasting models, sea surface wind speed and significant wave height follow a monotonical relationship under a growing sea up to the fully developed stage. This final stage is usually reached when the phase velocity corresponding to the dominant peak wave slightly exceeds the wind speed. The significant wave heights for fully developed seas were proposed by various authors, for example, Sverdrup and Munk (1947), Neumann (see Kinsman 1965), Pierson and Moskowitz (1964), Ewing and Laing (1987), and Hasselmann et al. (1988). Among these relationships, the Wave Model (WAM)-derived expression is found to have an intermediate overall growth rate for wind speed ranging from 0 to 30 m s^{-1} (see Pierson 1991), and is therefore chosen for our analysis.

Based on the WAM model (Hasselmann et al. 1988), the wind–wave relation for fully developed seas can be expressed as

$$H = 1.614 \times 10^{-2}U^2 \quad (0 \le U \le 7.5 \text{ m s}^{-1}) \tag{1a}$$

$$H = 10^{-2}U^2 + 8.134 \times 10^{-4}U^3 \quad (7.5 \text{ m s}^{-1} < U \le 50 \text{ m s}^{-1}), \tag{1b}$$

where U (in m s^{-1}) is the wind speed at 10-m height, and H (in m) is the significant wave height (Pierson 1991). A graphic illustration of Eq. (1) is shown in Fig. 1 (the thick curve), along with coincident measurements of wind speed from NSCAT/QSCAT and significant wave height from TOPEX (see section 2b). The Pierson and Moskowitz (1964) and the Ewing and Laing (1987) wind–wave relations are also included in Fig. 1 for reference. A direct implication of this graph is that the fully developed relationship may be used as a dividing line for sea state maturity: Measurements lying below the curve are mostly from a growing sea, while those above the curve are probably swell dominated. Of course this inference is not supposed to be valid in an absolute sense due to the complexity of the wind wave–swell coupling. But it is expected to give a meaningful classification of the two regimes from a statistical point of view.

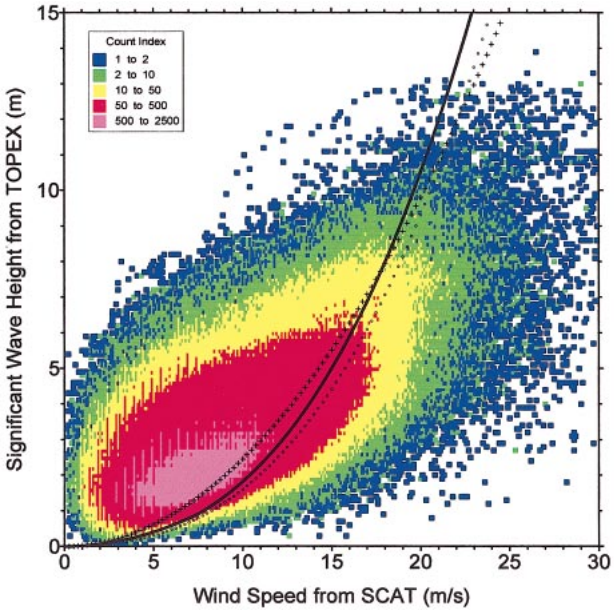

FIG. 1. A scatter diagram of sea surface wind speed and significant wave height based on the collocated TOPEX/NSCAT and TOPEX/QSCAT datasets. The wind speeds are extracted from NSCAT and QSCAT, and the significant wave heights are extracted from TOPEX. The color legend depicts data density. Also overlaid are the theoretical relations between wind speed and significant wave height for fully developed seas according to Hasselmann et al. (1988) (the WAM model), Pierson and Moskowitz (1964), and Ewing and Laing (1987), as depicted by the solid line, the crosses, and the circles, respectively.

5. Summary

Knowledge on the global structure of swell and wind sea probabilities in a climatological sense is believed to be generally poor to date. This study represents the first of its kind toward a better understanding of these important parameters. It has benefited from the availability of simultaneous multisatellite missions, which provide independent measurements of wind speed and significant wave height with unprecedented accuracy. Using the two energy-based indices proposed in this study, the global distribution and seasonal variation of swell and wind sea climate of the ocean is investigated. As a summary, the identified major swell pools (in red) and wind wave zones (in blue) in the world's oceans are indicated in Fig. 7. Given the reasonable results obtained in this study and their general consistency with available field observations and model predictions, the proposed scheme appears to be effective and efficient in characterizing the global swell and wind sea climate. Further exploration based on this feasibility study with longer duration of collocation dataset (which can be readily achievable by incorporating simultaneous TOPEX/ERS measurements as well as other forthcoming concurrent altimeter/scatterometer missions) will undoubtedly lead to a more realistic and more complete description of the swell and wind sea conditions in the ocean, in particular their interannual variabilities on a decadal timescale.

A rapidly declining perennial sea ice cover in the Arctic

Josefino C. Comiso

Laboratory for Hydrospheric Processes, NASA Goddard Space Flight Center, Greenbelt, Maryland, USA

Received 11 June 2002; revised 13 August 2002; accepted 28 August 2002; published 18 October 2002.

[1] The perennial sea ice cover in the Arctic is shown to be declining at −9% per decade using satellite data from 1978 to 2000. A sustained decline at this rate would mean the disappearance of the multiyear ice cover during this century and drastic changes in the Arctic climate system. An apparent increase in the fraction of second year ice in the 1990s is also inferred suggesting an overall thinning of the ice cover. Surface ice temperatures derived from satellite data are negatively correlated with perennial ice area and are shown to be increasing at the rate of 1.2 K per decade. The latter implies longer melt periods and therefore decreasing ice volume in the more recent years. *INDEX TERMS:* 4207 Oceanography: General: Arctic and Antarctic oceanography; 4215 Oceanography: General: Climate and interannual variability (3309); 1635 Global Change: Oceans (4203); 1640 Global Change: Remote sensing. **Citation:** Comiso, J. C., A rapidly declining perennial sea ice cover in the Arctic, *Geophys. Res. Lett.*, *29*(20), 1956, doi:10.1029/2002GL015650, 2002.

1. Introduction

[2] The Arctic sea ice cover has been noted as basically impenetrable because of the dominant presence of the perennial ice cover that consists mainly of multiyear ice, the average thickness of which is about 3–4 meters [*Wadhams and Comiso*, 1992]. The thick multiyear ice floes are the major components of the current Arctic sea ice cover. Their presence during the peak of summer makes a big difference in the ocean-ice-albedo feedback because of their vast extent and high albedo. They survive the summer melt mainly because of a strongly stratified Arctic Ocean that is in part responsible for the scarcity of convection in the region [*Aagard and Carmack*, 1994]. A study of the perennial ice cover is of immense practical importance because of the potential impact not only on climate but also on the environment and ecology of the system and in light of recent reports of ice retreat [*Bjorgo et al.*, 1997; *Parkinson et al.*, 1999] and ice thinning [*Rothrock et al.*, 1999; *Wadhams and Davis*, 2000].

[3] In this paper, the state of the perennial sea ice cover is studied using satellite passive microwave data from 1978 through 2000. The multiyear ice cover has been inferred from passive microwave data in winter using a technique that assumes that the signature is spatially stable during this period [*Johannessen et al.*, 1999]. However, previous studies have indicated large regional variations in the passive microwave signature [*Grenfell*, 1992] causing substantial biases in the derived fraction of multiyear ice within the pack [*Kwok et al.*, 1996]. The key to a more accurate quantification of the multiyear ice cover is through the use of data during minimum extent since at this time, the seasonal sea ice cover has basically melted and what is left is what we call the perennial ice cover consisting mainly of multiyear ice floes [*Comiso*, 1990]. These data are also easier to quantify and interpret since no ice classification is needed.

0094-8276/02/2002GL015650$05.00

2. Spatial Variability in the Perennial Sea Ice Cover

[4] To provide an overview about interannual variations in the spatial distribution of the perennial ice cover, color-coded ice concentration maps during the summer ice minimum from 1979 to 2000 are shown in Figure 1. The ice concentration maps were derived from satellite passive microwave data using the Bootstrap Algorithm as described in *Comiso et al.* [1997]. Slight adjustments were made to ensure that the data set is temporally consistent using a procedure similar to that used in *Parkinson et al.* [1999]. The day of minimum extent for each year is determined through the use of seven-day running mean data of ice extents. The running mean is used to maximize the chance that what is chosen is the date of real minima and not what might be the result of a temporary compaction due to wind forcing. The dates are mainly in the second or third week of September (Figure 1) and are found to be consistent within a few days with those of ice area minimum.

[5] The images in Figure 1 provide a means to quantitatively identify the relative location and concentration of multiyear ice floes at the end of each ice season. The open water area (blue) around the pack is shown to vary considerably from one year to the next. The circular black areas in the middle are areas not covered by the satellite sensors but are usually highly consolidated. The general location of the perennial sea ice cover changes from one year to another and depends on many factors, the most important of which is the ice drift which has been shown to be strongly influenced by atmospheric circulation [*Thorndike and Colony*, 1982]. The latter can be in cyclonic mode in which the ice is normally advected to the west causing large open water areas in the east (e.g., Laptev and Kara Seas) and relatively small open areas in the west (e.g., Beaufort Sea and Chukchi Seas) or in anti-cyclonic mode in which the opposite scenario occurs. Examination of the images in Figure 1 also indicates that the open water areas are generally larger in the 1990s than in the 1980s.

[6] To better illustrate the changes from one decade to another, Figure 2a shows the average of the ice concentration minimum maps from 1979 to 1989 while Figure 2b shows the corresponding average from 1990 to 2000. It is apparent that the size of the ice cover in the latter period is smaller than that of the earlier one and that much of the changes occurred around the ice margin. The changes from

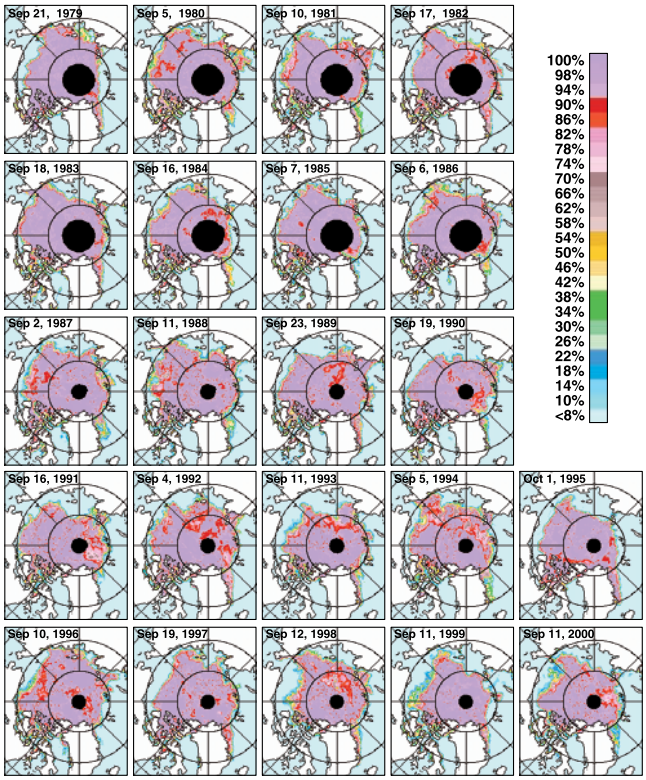

Figure 1. Color-coded daily ice concentration maps in the Arctic during ice extent minima for each year from 1979 to 2000. Each map represents the state of the perennial ice cover at the end of the ice season.

one decade to another are better quantified in the difference map (Figure 2c) between the two ice concentration maps. This map shows the magnitude and location of the changes with the negative changes represented by yellows, oranges, purples and reds while positive changes are in grays, greens, and blues. The interdecadal change is surprisingly large and intriguing with the net negative changes in extent and ice area being 5.1×10^5 km^2 (6.3%) and 6.9×10^5 km^2 (11.0%), respectively, during the 22-year period. The biggest change occurred in the western area (Beaufort and Chukchi Seas) while considerable changes are also apparent in the eastern region (Siberian, Laptev and Kara Seas). To get an idea how the ice cover may look like 5 decades from now, the decadal change as reflected in Figure 2c (but shifted towards the north) is applied to the data in Figure 2b and subsequent projections, normalized such that the change is about 10% per decade. The projected perennial ice cover for the decade of the 2050s is shown in Figure 2d. Although the technique is crude and the assumption of a linear decline is likely incorrect, Figure 2d provides a means to assess how the perennial ice cover could look like if the decline persists. It is important to note that the Arctic is governed by complex processes including a positive ice-ocean-atmosphere feedback and decadal as well as interdecadal variability including that associated with the Arctic Oscillation (AO) as described by [*Thompson and Wallace*, 1998]. A simple regression analysis of AO indices with the perennial ice area indicates that the relationship between these two variables is relatively weak with the correlation coefficient being only 0.20. The link is likely stronger if continuous ice cover data are analyzed in conjunction with the AO but such study is not within the scope of this paper.

4. Discussion and Conclusions

[13] The area of the Arctic perennial sea ice cover is shown to be declining at a relatively fast rate of 8.9 ± 2.0% per decade. A decadal change of 10% is also inferred from the difference of 11-year averages of ice minima data. If such a rate of decline persists for a few more decades, the perennial sea ice cover will likely disappear within this century. The decline is unlikely linear because of positive feedback effects between ice, ocean, and the atmosphere Furthermore, a positive trend in the ice temperature of about 1.2 K per decade is observed leading to earlier onset of melt and delayed onset of freeze up that in turn causes further thinning and retreat of the perennial ice cover.

[14] The implications of such a disappearance of the perennial ice cover are many and can be profound. It would mean a different albedo for the Arctic during the peak of solar insolation in summer and therefore a drastically different ice-ocean-atmosphere feedback. It would mean a much larger influx of solar radiation into the Arctic Ocean thereby changing the characteristics of the mixed layer and the stratification of the ocean. The seasonality and characteristics of the ice cover in the region would be very different. The climate, the productivity, and biota in the region will change tremendously while the region becomes more accessible to human activities.

[15] The Arctic system is however a complex system controlled by many variables and influenced by unpredictable events (e.g., volcanic eruptions). There are also periodic cycles, such as the Arctic Oscillation [*Thomson and Wallace*, 1998], the North Atlantic Oscillation [*Mysak and Venegas*, 1998] and the Pacific Decadal Oscillation [*Chao et al.*, 2000] the effects of which need to be considered. The associated decadal and inter-decadal changes in pressure and atmospheric circulation could cause a decadal variability in the ice cover that could lead to a reversal in the current trend. Nevertheless, because of the magnitude in the observed rate of decline and associated feedback effects, a near term recovery is likely needed to avoid an irreversible change in the Arctic ice cover and its environment.

Annals of Glaciology 34 2002

Correlation and trend studies of the sea-ice cover and surface temperatures in the Arctic

JOSEFINO C. COMISO
Laboratory for Hydrospheric Processes, NASA Goddard Space Flight Center, Code 971, Greenbelt, MD 20771, U.S.A.

ABSTRACT. Co-registered and continuous satellite data of sea-ice concentrations and surface ice temperatures from 1981 to 2000 are analyzed to evaluate relationships between these two critical climate parameters and what they reveal in tandem about the changing Arctic environment. During the 19 year period, the Arctic ice extent and actual ice area are shown to be declining at a rate of $-2.0 \pm 0.3\%$ dec^{-1} and $-3.1 \pm 0.4\%$ dec^{-1}, respectively, while the surface ice temperature has been increasing at 0.4 ± 0.2 K dec^{-1}, where dec is decade. The extent and area of the perennial ice cover, estimated from summer minimum values, have been declining at a much faster rate of $-6.7 \pm 2.4\%$ dec^{-1} and $-8.3 \pm 2.4\%$ dec^{-1}, respectively, while the surface ice temperature has been increasing at 0.9 ± 0.6 K dec^{-1}. This unusual rate of decline is accompanied by a very variable summer ice cover in the 1990s compared to the 1980s, suggesting increases in the fraction of the relatively thin second-year, and hence a thinning in the perennial, ice cover during the last two decades. Yearly anomaly maps show that the ice-concentration anomalies are predominantly positive in the 1980s and negative in the 1990s, while surface temperature anomalies were mainly negative in the 1980s and positive in the 1990s. The yearly ice-concentration and surface temperature anomalies are highly correlated, indicating a strong link especially in the seasonal region and around the periphery of the perennial ice cover. The surface temperature anomalies also reveal the spatial scope of each warming (or cooling) phenomenon that usually extends beyond the boundaries of the sea-ice cover.

INTRODUCTION

The Arctic region is of particular interest because it is expected to provide early signals associated with a potential change in climate (Budyko, 1966; Manabe and others, 1992; Alley, 1995). Because of observed global warming, especially in the second half of the 1990s (Jones and others, 1999), it is important to know how such increases in temperature are reflected in the Arctic. Recent reports show that the sea-ice cover has been retreating by about -3% dec^{-1} (Bjørgo and others, 1997; Parkinson and others, 1999), while submarine sonar data show a thinning by >1 m in deep-water portions of the Arctic (Rothrock and others, 1999; Wadhams and Davis, 2000) over a period of 4 dec, where dec is decade. The Arctic climate system is, however, a very complex system affected by periodic atmospheric phenomena, like the North Atlantic and Arctic Oscillations (Mysak, 1999), and unexpected changes in ice-cover dynamics. Accurate interpretation of observed Arctic changes thus requires a better understanding of Arctic processes.

The key objective of this study is to make simultaneous use of satellite sea-ice concentration and surface temperature data to gain insight into the changing Arctic climate. Co-registered datasets of these two geophysical variables are examined to obtain a better understanding of how the various components of the climate system interact and how they act in concert to influence the system. Previous studies on the variability and trends of the Arctic sea-ice cover have been carried out using solely satellite passive-microwave data or submarine sonar data. In this study, trends and spatial changes in the ice cover are analyzed in conjunction with trends and changes in surface temperatures. Anomalies in ice concentration and surface temperatures are examined on a year-to-year basis, and relationships between these two variables are evaluated. The results are also used to gain insight into the observed changes in the Arctic, interpret trends in the total ice cover and its surface temperature, and better understand the status of the perennial sea-ice cover.

VARIABILITY AND TREND OF THE SEA-ICE COVER

Although a slightly longer time series for sea-ice cover is available, the time period used in this study is 1981–99 since this is the period for which coincident and continuous infrared and passive-microwave satellite data are available. The procedure for deriving ice concentration from satellite passive-microwave data has been described before (Comiso and others, 1997) and will not be repeated here. The error associated with the ice-concentration data is about 5–15% under dry surface conditions, and increases when the surface becomes wet as the snow melts in spring and when melt ponds are formed over ice floes in the summer. In this study, the ice concentrations are derived using the Bootstrap algorithm as described in Comiso and others (1997). The values and trends may therefore be slightly different from those reported elsewhere (Bjørgo and others 1997; Parkinson and others, 1999) even for identical periods.

Ice-concentration maps are used to derive monthly ice extent, actual ice area and average ice concentrations within the pack, as done previously (Comiso and others, 1997; Parkinson and others, 1999). These are in turn used to calculate anomalies in monthly ice extent, actual ice area and ice concentration by subtracting the 19 year climatological

averages created for each of the 12 months of the year. The anomalies in ice extent, ice area and ice concentration for each month from August 1981 through July 2000, which are also used for trend studies, are shown in Figure 1. Yearly averages were also calculated for analysis of the yearly variability and associated trend. The yearly averaging was done from August of one year to July the following year to be able to compare yearly differences between different ice seasons, instead of different annual averages that would extend from the middle of one ice season to the middle of another.

The plot of ice-extent anomalies (Fig. 1a) shows significant variability, with a standard deviation of 0.33×10^6 km^2. Simple linear regression of the data yielded a trend of $-246\,000 \pm 40\,000$ km^2 dec^{-1}, or $-2.04 \pm 0.33\%$ dec^{-1}. This is significantly less than the -2.8% dec^{-1} reported by Parkinson and others (1999), but the latter was for a slightly different time period (i.e. 1978–96) and a different ice dataset was used (i.e. Team algorithm as described in Comiso and others, 1997), as indicated earlier. Anomalously low values occurred in 1989, 1990, 1993, 1995 and 1998, while an anomalously high value is apparent in 1996. The regression results from the yearly data yielded $-2.04 \pm 0.56\%$ dec^{-1} the result of which is almost the same as the monthly anomaly data but with higher error.

The variability in the anomalies in actual ice area (Fig. 1b) is comparable to that of ice extent, with a standard deviation of 0.33×10^6 km^2. However, the trend in ice area is significantly larger at $-336\,000 \pm 36\,000$ km^2 dec^{-1}, or $-3.11 \pm 0.33\%$ dec^{-1}. This is more in line with previous reports for the 1978–96 period. The yearly averages yielded similar trends but larger error at $-3.12 \pm 0.51\%$ dec^{-1}.

The difference between the ice-extent and ice-area trends stems mainly from a net negative trend in ice concentration (Fig. 1c), estimated at $-1.16 \pm 0.12\%$ dec^{-1}. The change in estimated ice concentration may not be entirely due to a change in true ice concentration since it could also be linked to a change in the areal coverage of melt ponding. To test this possibility, a similar analysis was conducted that excluded the summer months (June–August). The results yielded a trend in ice concentration of $-1.09 \pm 0.14\%$ dec^{-1}, which is similar to that with the summer months included. This implies that the impact of changes in melt-ponded area on the trend results is not significant. However, excluding the summer months significantly reduced the trends in ice extent and area to $-1.47 \pm 0.14\%$ dec^{-1} and $-2.47 \pm 0.37\%$ dec^{-1}, respectively. This suggests that the trends in the ice cover during the summer, especially during minima, may be high as indicated later.

The distributions for the yearly average extent and area in Figure 1 exhibit a periodic cycle with a period of about 5 years. Such periodicity is intriguing in light of a possible correlation with many important processes, such as the Arctic Oscillation. The effect is not so apparent in the monthly anomalies. However, a detailed study of this phenomenon is beyond the scope of this paper.

DISCUSSION AND CONCLUSIONS

Co-registered satellite ice-concentration and surface-temperature data for the period 1981–2000 have been assembled and analyzed, and this study shows that simultaneous observation of the two parameters provides useful knowledge about the changing Arctic. Ice-concentration data provide physical characterization of sea-ice spatial distributions, while surface temperatures provide information about the thermal state of the ice surface. Each dataset provides independent evaluation of the changing state of the Arctic, but together they provide a more complete characterization.

A general assessment from the monthly and yearly data shows that ice extent has been declining at a rate of 2.3% dec^{-1} while surface temperature has increased by 0.4 K dec^{-1}. This rate of decline is smaller than the 2.8% dec^{-1} previously reported, but that value was for a different period (1978–96) and a different ice-concentration algorithm was utilized to generate the ice dataset.

The yearly anomalies in both ice concentration and temperature provide new insights into the changing Arctic ice environment. They provide year-to-year changes in good spatial detail of sea-ice distributions, and specific locations and magnitude of large positive and negative anomalies. The data show that positive anomalies in ice concentrations predominate in the 1980s, while the reverse is true in the 1990s. This indicates that the ice cover has been declining. Similarly, negative anomalies in surface temperatures were dominant in the 1980s, while positive anomalies were more frequent in the 1990s. This shows that while the ice cover is declining, the surface temperature is rising, indicating a close linkage of the two variables.

The yearly temperature-anomaly maps provide useful information that is not available from the sea-ice-cover data. These maps show that there are large anomalies in the Arctic that extend beyond the sea-ice margins. They allow quantification of the scope of these anomalies which are apparently driven by atmospheric patterns. The coherence of the spatial distribution of the anomalies of ice concentration and surface temperature is quite good, and quantitative analysis shows high negative correlation of the two variables, especially in the seasonal ice regions where the anomalies are abnormally high. It is also apparent that there were some years when the anomaly patterns were exceptionally high, such as 1998, which is regarded as the warmest year in the 20th century. High positive anomalies are indeed evident in the 1997/98 and 1998/99 ice seasons, but they are confined primarily to the Beaufort Sea and North America, while slight cooling occurred in Russia and the Kara Sea.

To better understand the current state of the Arctic ice cover, a good quantification of the variability of the perennial ice cover is required, derived from analysis of the extents and areas of the ice cover during summer minimum. Results show that the Arctic summer ice extent and area have been declining at a rate of $-6.7 \pm 2.4\%$ dec^{-1} and $-8.3 \pm 2.4\%$ dec^{-1}, respectively, while the average September surface temperature values increased by 0.9 ± 0.6 K dec^{-1}. The rate of decline in the perennial ice cover is more than twice the rate of decrease in total sea-ice cover. The rate of increase in surface temperature in September is also surprisingly high and more than double that for all seasons. These are significant results since they pertain to the perennial ice cover which is directly connected to the ice-thickness distribution. In addition, the minimum extent shows higher yearly fluctuations in the 1990s than in the 1980s. Even without a trend, such a phenomenon would cause a change in the overall composition of the different ice types, and favors increases in the fraction of the thinner, younger ice cover (e.g. second-year ice), compared with the older, thicker ice types. The large fluctuation in the areal coverage of the perennial ice cover may thus be accompanied by a decrease in ice thickness.

WEATHER MAGAZINE

May/June ISSUE, 2002

Abstract

A state that ranks 42nd in size, Maryland has taken an inordinate number of tornado hits--two of them deadly. On Sep 24, 2001, an F3 twister took the lives of two students as it ripped through the University of Maryland at College Park. On Apr 28, 2002, an F4 tornado killed five people and devastated the town of La Plata. During the first half of May 2002, three different twisters and several downbursts pounded various parts of the state.

MAY HIGHLIGHT

Twisters Claw Maryland

by James Foster

JAMES FOSTER is a lifelong Maryland resident and a climatologist in the Hydrological Sciences Branch at NASA's Goddard Space Flight Center in Greenbelt, Maryland.

Many of us can recall our grandparents regaling us with stories about what the weather was like when they were growing up. Gramps would say something like, "Back in '32, the winter was so long that I had to put snowshoes on both me and the mule to plow the north 40."

We listened in amazement and wondered what it must have been like back then. Sometimes you've got to wonder if it really was that much worse. Chances are, Gramps was remembering a cluster of bad weather events that made the extremes seem even more extreme.

Take the past couple of years in Maryland, for example. A state that ranks 42nd in size, Maryland has taken an inordinate number of tornado hits—two of them deadly. Almost a year ago, on September 24, 2001, an F3 twister took the lives of two students as it ripped through the University of Maryland at College Park.

And this past spring, on April 28, an F4 tornado killed five people and devastated the town of La Plata, 30 miles south of Washington, D.C. If that wasn't bad enough, during the first half of May, three different twisters and several downbursts pounded various parts of the state.

Maryland residents have become more attuned to just how dangerous tornadoes can be and are taking tornado warnings more seriously, sometimes to the point of dramatically overreacting. In fact, about a week after the La Plata tornado occurred, an adjacent county closed schools when a tornado watch was issued.

The La Plata tornado was a product of a supercell thunderstorm that formed ahead of a cold front pushing east across the Ohio Valley. April 28 was warm and very humid across the mid-Atlantic. Dew points in Washington, D.C., were in the low 70s (°F), and temperatures rose to the upper 70s once the sun emerged after heavy morning rain. Wet ground, moist air, and warm temperatures helped to fuel the development of afternoon thunderstorms. Moreover, the jet stream, positioned over the mid-Atlantic region, acted to intensify the developing storms.

An energetic cold front can act as a triggering mechanism for tornado formation if a large area of moisture is surging north from the Gulf of Mexico and if a vigorous jet stream is positioned overhead. Because of the very unstable atmosphere, the National Weather Service issued tornado watches and severe thunderstorm warnings well before the first funnel cloud was sighted.

Even by "Tornado Alley" standards, the La Plata tornado was big. After demolishing La Plata, it hit Prince Frederick, Maryland, and then hopscotched across the Chesapeake Bay onto Maryland's Eastern Shore. The storm cell associated with the deadly La Plata tornado persisted all the way from the Appalachians to the Atlantic Ocean.

Maryland's most deadly tornado disaster also occurred near La Plata 76 years ago when a schoolhouse was demolished and more than a dozen children were killed.

While little Maryland has recently been battered by a number of unwelcome twisters, most of the rest of the country has dodged them. In fact, for the last two years and thus far this year, the number of reported tornadoes nationwide has been below the 30-year mean.

So, why then has Maryland had to deal with more than its share of tornadoes? Basically, it's just by chance that the cast of meteorological characters that must appear on stage at the same time to produce the fiercest winds on Earth has done so with some regularity in Maryland. The show is usually seen in the southern Plains and the Midwest, but over the past year, it went on the road to the east. As always, the reviews were dreadful. The bottom line is that Maryland needn't worry about becoming a new "Tornado Alley," though it may have seemed so recently.

Nonetheless, I suppose in 50 years, today's kids will be telling their grandchildren what it was like when they were young sprouts. "Back in '02, you didn't even have to till your fields in the spring; the twisters came so thick and fast, you'd just wait for one of them to plow up the ground for you."

An aerial view of the 10-mile swath that the tornado left behind in La Plata, Maryland, in late April. The remains of La Plata appear at the left, where the tornado path crossed the north-to-south Route 301.
COURTESY OF EO-1 SCIENCE TEAM, NASA GODDARD SPACE FLIGHT CENTER

Southern Ocean Climate and Sea Ice Anomalies Associated with the Southern Oscillation

R. KWOK

Jet Propulsion Laboratory, California Institute of Technology, Pasadena, California

J. C. COMISO

NASA Goddard Space Flight Center, Greenbelt, Maryland

(Manuscript received 5 February 2001, in final form 7 August 2001)

ABSTRACT

The anomalies in the climate and sea ice cover of the Southern Ocean and their relationships with the Southern Oscillation (SO) are investigated using a 17-yr dataset from 1982 to 1998. The polar climate anomalies are correlated with the Southern Oscillation index (SOI) and the composites of these anomalies are examined under the positive (SOI $>$ 0), neutral (0 $>$ SOI $>$ -1), and negative (SOI $<$ -1) phases of SOI. The climate dataset consists of sea level pressure, wind, surface air temperature, and sea surface temperature fields, while the sea ice dataset describes its extent, concentration, motion, and surface temperature. The analysis depicts, for the first time, the spatial variability in the relationship of the above variables with the SOI. The strongest correlation between the SOI and the polar climate anomalies are found in the Bellingshausen, Amundsen, and Ross Seas. The composite fields reveal anomalies that are organized in distinct large-scale spatial patterns with opposing polarities at the two extremes of SOI, and suggest oscillations that are closely linked to the SO. Within these sectors, positive (negative) phases of the SOI are generally associated with lower (higher) sea level pressure, cooler (warmer) surface air temperature, and cooler (warmer) sea surface temperature in these sectors. Associations between these climate anomalies and the behavior of the Antarctic sea ice cover are evident. Recent anomalies in the sea ice cover that are clearly associated with the SOI include the following: the record decrease in the sea ice extent in the Bellingshausen Sea from mid-1988 to early 1991; the relationship between Ross Sea SST and the ENSO signal, and reduced sea ice concentration in the Ross Sea; and the shortening of the ice season in the eastern Ross Sea, Amundsen Sea, far western Weddell Sea and lengthening of the ice season in the western Ross Sea, Bellinghausen Sea, and central Weddell Sea gyre during the period 1988–94. Four ENSO episodes over the last 17 years contributed to a negative mean in the SOI (-0.5). In each of these episodes, significant retreats in ice cover of the Bellingshausen and Amundsen Seas were observed showing a unique association of this region of the Antarctic with the Southern Oscillation.

1. Introduction

The Southern Oscillation (SO) refers to the seesaw in the surface pressure anomalies between the Indian Ocean–Australian region and the southeastern tropical Pacific on a seasonal and interannual timescale. The large-scale character of the SO in the Tropics and subtropics in the Southern Hemisphere is well known (Philander and Rasmusson 1985). The SO has a signature that extends to the mid- and high latitudes in the Southern Hemisphere in the winter and summer. The high-latitude signature of the SO has associated anomalies over the Antarctic sea ice cover. Understanding these links between the SO and Antarctic sea ice cover are important due to the sensitivity of sea ice to anomalies in climate forcing as sea ice interacts with the global climate over a broad range of spatial and temporal scales (Schlesinger and Mitchell 1985; Manabe et al. 1991). Sea ice albedo feedback involves changes in the climatological area of the ice cover and adjustments in the poleward heat transport by the atmosphere, in addition to changes in the thickness, albedo, and temperature of ice within the Antarctic ice pack. The ocean structure and circulation are affected during sea ice growth, as salt is rejected to the underlying ocean increasing its density and leading sometimes to deep ocean convection and bottom water formation. Equatorward transport of ice results in a net flux of freshwater and negative heat. Thus, anomalies in these polar processes have complex consequences in the global climate.

Many studies have analyzed the recent behavior of the Antarctic ice extent and have suggested connections between sea ice extent and the Southern Oscillation (Carleton 1988; Jacobs and Comiso 1993; Simmonds and Jacka 1995; Gloersen 1995; Ledley and Huang 1997; Jacobs and Comiso 1997; Watkins and Simmonds 2000). Using a 10-yr dataset (1985–94), White and Peterson (1996) found coupled anomalies that propagate eastward with the Antarctic Circumpolar Current during a period of 4–5 years (wavenumber 2) and taking 8–10 years to encircle Antarctica. It was suggested that this Antarctic Circumpolar Wave (ACW) is associated with ENSO-related activities in the equatorial Pacific, possibly through an atmospheric teleconnection with higher southern latitudes. Peterson and White (1998), in a case study, show ENSO can be a possible source of the interannual anomalies for sustaining the ACW in the western subtropical South Pacific. Parkinson (1998) also

Corresponding author address: Dr. R. Kwok, Jet Propulsion Laboratory, California Institute of Technology, 4800 Oak Grove Dr., Pasadena, CA 91109.
E-mail: ron.kwok@jpl.nasa.gov

suggests that the lengthening/shortening sea ice season might be related to the variability of the ACW. Bonekamp et al. (1999) in an examination of the European Centre for Medium-Range Weather Forecasts (ECMWF) Atmospheric Reanalysis dataset from 1979 to 1994, however, did not find eastward propagating anomalies suggestive of an ACW prior to 1984. For that time period at least, a two-regime structure with and without the presence of ACW was indicated. Yuan and Martinson (2000) explored possible relationships between the record of Antarctic sea ice extent between 1978 and 1996 and global climate variability. Their analyses show a strong link of the sea ice edge anomalies in the Amundsen, Bellingshausen, and Weddell Seas to extrapolar climate. In a recent article, Venegas et al. (2001) found coupled oscillations in Antarctic sea ice and atmosphere in the South Pacific sector.

The objective of this study is to explore the spatial details in the teleconnections between SO and the anomalies in the Southern Ocean climate and in particular the anomalies of the Antarctic sea ice cover. Our approach is to analyze the linear correlation of the Southern Oscillation index (SOI) with the polar climate anomalies, and to examine the composites of these anomalies during three phases of the SOI that we define as SOI > 0, $0 >$ SOI > -1, and SOI < -1, and henceforth will be referred to as the positive, neutral, and negative phases. The datasets used here span a 17-yr period from 1982 to 1998. Our study takes advantage of new data on ice motion and ice surface temperature derived from passive microwave imagery and the National Oceanic and Atmospheric Administration's (NOAA) Advanced Very High Resolution Radiometer (AVHRR) data. Rather than having to restrict our study area to the ice edge region, as was done previously (White and Peterson 1996), this dataset allows a more detailed examination of the spatial signatures of the climate and sea ice anomalies.

The paper is composed of five sections. Section 2 describes the climate and sea ice datasets used in our analysis. Section 3 presents the spatial pattern of correlation between the Southern Ocean climate anomalies and the SOI, and the composite patterns of the climate and sea ice anomalies associated with three phases of the SOI over 17 years. We discuss our results in the context of previous work in section 4. The paper is summarized in the last section.

5. Conclusions

The spatial signature of the climate and sea ice anomalies in the Southern Ocean associated with the Southern Oscillation are revealed in the correlation patterns and the composite fields. The correlation maps and lag-correlation plots show features of the spatial and temporal relationships between these anomalies and the index of Southern Oscillation, while the composite maps show the dominant spatial signature of the anomalies during the three phases of SOI. On a large scale, these anomalies are organized in coherent patterns and assume opposite polarities during the two extremes of SOI. Also, these anomalies covary with the Southern Oscillation and oscillate at approximately the same frequency. Association with ENSO-related activities in the equatorial Pacific is clearly indicated.

Overall, the climate anomalies in the Amundsen, Bellingshausen, and Weddell Sea sectors of the Antarctic polar ocean show the strongest link to the Southern Oscillation. Within these sectors, the climate anomalies show the highest correlation with the SOI and the composite patterns show the most intense and localized climate and sea ice anomalies associated with the extremes of SOI. Positive (negative) phases of the SOI are generally associated with lower (higher) sea level pressure, cooler (warmer) surface air temperature, and cooler (warmer) sea surface temperature in these sectors. Outside these sectors, the anomalies are not as distinct.

Linkages between the SOI, the climate anomalies, and the sea ice extent, concentration, motion, and ice surface temperature are also evident. The sea ice cover anomalies are located within the same sectors as those with the dominant climate anomalies. During the positive (negative) phase of SOI, positive (negative) anomalies of the SIE are located between 180° and 130°W in the Ross and Amundsen Seas, negative (positive) anomalies can be found between 100°W and 10°E in Bellingshausen and Weddell Seas, and, smaller positive (negative) anomalies are found in the sector between 10° and 50°E.

The physical mechanisms by which these polar processes are linked to the Southern Oscillation are complex and beyond the scope of this study. However, the identified relationships may be useful as diagnostic tools for climate models and for the eventual understanding of the underlying mechanisms of these associations. The composite fields presented can be used as an indicator of the general condition of the Antarctic ice cover during different phase of the Southern Oscillation as measured by the SOI. We have used these fields to explain, in a broad sense, the large-scale trends and anomalies (reported in recent literature) in the sea ice extent and the length of the ice seasons over the past 20 years. These composite fields are weighted by four strong ENSO episodes over the last 17 years. As a result, these warm events have probably weighted the sea ice and climate anomalies towards the patterns associated with the negative extremes of the SO index. Data of monthly anomalies of ice extent, ice area, and concentration in the Bellingshausen–Amundsen Sea sector (Fig. 9) show that the ice cover in the region is still declining while those in other regions appear to be increasing slightly. In fact, the mean trend of the Antarctic sea ice edge is close to zero over the period. Recession of the ice edge in the Bellingshausen–Amundsen Sea sector is compensated by expansion in the Weddell Sea and western Ross Sea sectors. Our analysis shows that spatially, the Pacific sector is different from other Antarctic regions in that it is influenced by climate anomalies with strong associations with the Southern Oscillation. The results suggest that the Bellingshausen–Amundsen Sea area is unique in its close association with the Southern Oscillation.

Spatial patterns of variability in Antarctic surface temperature: Connections to the Southern Hemisphere Annular Mode and the Southern Oscillation

Ron Kwok
Jet Propulsion Laboratory, California Institute of Technology, Pasadena, California, USA

Josefino C. Comiso
Goddard Space Flight Center, Greenbelt, Maryland, USA

Received 1 May 2002; revised 7 June 2002; accepted 14 June 2002; published 31 July 2002.

[1] The 17-year (1982–1998) trend in surface temperature shows a general cooling over the Antarctic continent, warming of the sea ice zone, with moderate changes over the oceans. Warming of the peripheral seas is associated with negative trends in the regional sea ice extent. Effects of the Southern Hemisphere Annular Mode (SAM) and the extrapolar Southern Oscillation (SO) on surface temperature are quantified through regression analysis. Positive polarities of the SAM are associated with cold anomalies over most of Antarctica, with the most notable exception of the Antarctic Peninsula. Positive temperature anomalies and ice edge retreat in the Pacific sector are associated with El-Niño episodes. Over the past two decades, the drift towards high polarity in the SAM and negative polarity in the SO indices couple to produce a spatial pattern with warmer temperatures in the Antarctic Peninsula and peripheral seas, and cooler temperatures over much of East Antarctica. *INDEX TERMS:* 3309 Meteorology and Atmospheric Dynamics: Climatology (1620)

1. Introduction

[2] While global temperatures rose by 0.3°C between 1978–1997 [*Jones et al.*, 1999], the spatial distribution of this trend is certainly not uniform. During the last 20 years, pronounced warming of the Antarctic Peninsula [*King and Harangozo*, 1998] has been contrasted by reported cooling at a number of weather stations on the coast and plateau of East and West Antarctica [*Comiso*, 2000]. Recently, the analysis of *Doran et al.* [2002] suggests a net cooling of the Antarctic continent between 1966 and 2000. Over approximately the same period, the warming trend of 0.09°C/yr (1980–1999) at Faraday Station at the northern tip of the Antarctic Peninsula can be compared to the cooling trends of 0.07°C/yr (1986–2000) at the McMurdo Dry Valleys and 0.05°C/yr at the South Pole (1980–1999).

[3] Surface temperature (ST) anomalies of the Antarctic are related to anomalies in atmospheric and ocean circulation, and the sea ice cover. A new 17–year (1982–1998) ST dataset [*Comiso*, 2000] allows us to identify the characteristic spatial patterns of variability in the Antarctic ST field and their relation to large-scale circulation patterns. In this paper, we explore the linear effects of the SAM and the SO on the ST fields of the Antarctic. The SAM describes a predominantly zonally symmetric pattern and is characterized by sea-saws of atmospheric mass between the polar caps regions poleward of 60°S and the surrounding zonal ring centered along ~45°S, as manifested in the leading empirical orthogonal functions (EOFs) of the 850-hPa geopotential height field [*Thompson and Wallace*, 2002a]. This annular mode is also related to strong perturbations in temperature and total ozone column over the polar caps during the stratosphere's active season. Linkages between the well known SO, and the climate and sea ice anomalies of the Southern Ocean have been described by *Kwok and Comiso* [2002]. The SO plays a role in the regional pattern of Antarctic climate changes over the past 20-years. Here, the SO is discussed in the context of potential interactions between the two modes of atmospheric variability.

2. Data Sets and Circulation Indices

[4] The monthly ST fields used in this study are derived from AVHRR (A Very High Resolution Radiometer) infrared data. The dataset, on a 6.25 km grid, covers ocean and ice south of 50°S. STs at skin depth are generally close estimates of near surface air temperatures (SATs). In the extreme these temperatures maybe cooler by several degrees, compared to near SATs, under conditions with stable stratification over ice surfaces. As infrared observations of the surface are available only during cloud-free conditions, the temperatures may not properly reflect the monthly mean. When compared to monthly station data, the cloud-free averages are cooler than the true monthly mean by ~0.5 K. Details of the retrieval procedure and evaluation of the dataset can be found in *Comiso* [2000]. Uncertainties in the retrievals are estimated to be generally less than 3 K over ice-covered surfaces and less than 1 K over open ocean. The data are mapped onto the polar stereographic projection used in SSM/I (Special Sensor Microwave/Imager) data. Monthly anomaly ST fields are produced by removing the monthly climatology at each sample location.

[5] Indices of the SAM are those derived by *Thompson and Wallace* [2002a]. These are coefficients of the leading mode in the EOF expansion of the monthly 850-hPa geopotential height field, from 20–90S, [1958–1997] from the NCEP/NCAR Reanalysis [*Kalnay et al.*, 1996]. This mode explains ~27% of the variance of the monthly mean fields poleward of 20°S. The monthly SO indices used in this

0094-8276/02/2002GL015415$05.00

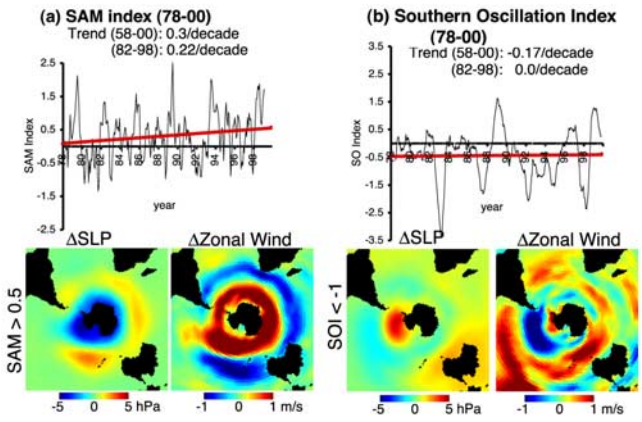

Figure 1. The indices of the SAM and the SO from 1978–2000, and the composites of SLP and zonal wind anomalies associated with their positive polarities (SAM index > 0.5; SO index < −1) of the indices. The SLP and wind anomalies are derived from NCEP/NCAR analyses. The trends (1958–2000) in the indices are also shown. The 17-year trend is shown in red.

study are those of the Climate Analysis Center. The time series of the two indices and the mean SLP and wind anomaly patterns associated with the positive polarity of the SAM and negative polarity of the SO indices are shown in Figure 1. The most striking features associated with the positive polarity of the SAM index are the lowered SLP within the circumpolar trough, enhancement of the westerlies north of 70°S, and negative anomalies in the meridional wind west of the Antarctic Peninsula. For the positive polarity of the SO, lowered SLP is found centered over the Amundsen and Bellingshausen Seas, with corresponding meridional and zonal wind anomalies. Opposite polarities of the SAM and SO indices exhibit the same spatial patterns but with anomalies of opposite sign.

3. Results and Discussion

[6] The 17-year (1982–1998) trends of the ST and ice edge (IE) anomalies are shown in Figure 2. The most pronounced feature on the map is the warming of the sea ice zone around Antarctica. It should be emphasized that the trend over sea ice should be interpreted with care, as the retrievals over sea ice are highly variable because the STs are dependent on ice thickness and concentration. The ST of thin ice is closer to the freezing point at the bottom boundary (sea water at ∼−1.8°C) while the ST of thick ice is closer to that of the SATs. With sea ice in the 0–1 meter range, as is typical in the Southern Ocean, there could be significant contrasts between ice and air temperatures. Ice concentration anomalies are results of openings and closings of the ice cover due to gradients in ice motion. Thus, the overall trend may be potentially interpreted as expressions of lower ice concentration and/or a thinner ice cover. In the warming over the Amundsen/Bellingshausen Seas, there are no significant trends in the sea ice concentration [*Kwok and Comiso*, 2002] but observations show significant negative trends in the IE (shown in Figure 1) and decreases in the sea ice season [*Parkinson*, 1998]. Thus, the increase in ST could be partially attributable to the increase the area of thinner first year ice in winter and longer periods with open water in summer. Regions with negative trend in the IE are coincident with areas with warming. The two sectors, west of the Ross Sea and east of the Antarctic Peninsula in the Weddell Sea, showing cooling trends are coincident with positive trends in the IE.

4. Conclusions

[12] Observed changes in the ST of the Antarctic appear to be linked to variations in the extratropical SH annular mode and the extrapolar Southern Oscillation. Spatially, it is clear from Figure 2 that the SAM and SO indices do not explain the same ST variances, as the two indices are almost uncorrelated. The SAM plays an important role in the circulation pattern and the spatial temperature distribution of the Antarctic sea ice and ice sheet. In surface temperature, positive (negative) polarities of the SAM indices are associated with the positive (negative) temperature anomalies over the Antarctic Peninsula and negative (positive) temperature anomalies over much of the continent. The regions of extremes in correlation with the SO indices are found in the SST fields off the Ross Sea (negative correlation) and sector off the George V and Oakes coasts (positive correlation). Warmer (cooler) SSTs off the Ross Sea is associated with the negative (positive) polarity of SO index, with the opposite behavior found in the other region. This analysis serves to illustrate the importance of the circulation changes associated with the SAM and SO in determining the spatial pattern of surface temperature anomalies.

[13] The upward trend in the SAM index accounts partially for the observed warming over the Antarctic Peninsula during the past 17-years while the negative bias in the SO index accounts for the retreat of the ice edge in the Bellingshausen Sea west of the Antarctic Peninsula. The significant and prolonged positive trend and bias in the difference between the SAM and SO indices (positive SAM and negative SO) during the past 17-years gave rise to this regional pattern with positive ST anomaly and reduced sea ice cover. We suggest perhaps that the total observed warming of the Antarctic Peninsula can be associated with the potential coupling of the modes of atmospheric variability described by the two indices through regional positive temperature/sea ice feedback. Regardless of the cause, the changes in the circulation since the early 80s have resulted in a particular ST anomaly pattern that has amplified warming of the Antarctic Peninsula because of the interactions between ice and ocean.

[14] The source of variability of the SAM has not been established. It is interesting to note that the variability of the tropospheric SH annular mode has been shown to be related to changes in the lower stratosphere [*Thompson and Wallace*, 2000b]. The high index polarity of the SH annular mode is associated with the trend toward a cooling and strengthening of the SH stratospheric polar vortex during the stratosphere's relatively short active season in November, and ozone depletion. A causal mechanism was suggested by recent Antarctic data showing a strong cooling trend in the lower stratosphere that is consistent with recent ozone depletions [*Randel and Wu*, 1999]. However, the primary mechanism responsible for the recent trend in the SH annular mode remains to be determined.

Annals of Glaciology 34 2002

A 21 year record of Arctic sea-ice extents and their regional, seasonal and monthly variability and trends

CLAIRE L. PARKINSON, DONALD J. CAVALIERI
Oceans and Ice Branch/Code 971, NASA Goddard Space Flight Center, Greenbelt, MD 20771, U.S.A.

ABSTRACT. Satellite passive-microwave data have been used to calculate sea-ice extents over the period 1979–99 for the north polar sea-ice cover as a whole and for each of nine regions. Over this 21 year time period, the trend in yearly-average ice extents for the ice cover as a whole is $-32\,900 \pm 6100$ km^2 a^{-1} (-2.7 ± 0.5% per decade), indicating a statistically significant reduction in sea-ice coverage. Regionally, the reductions are greatest in the Arctic Ocean, the Kara and Barents Seas and the Seas of Okhotsk and Japan; and seasonally, the reductions are greatest in summer, for which season the 1979–99 trend in ice extents is $-41\,600 \pm 12\,900$ km^2 a^{-1} (-4.9 ± 1.5% per decade). On a monthly basis, the reductions are greatest in July and September for the north polar ice cover as a whole, in September for the Arctic Ocean, in June and July for the Kara and Barents Seas, and in April for the Seas of Okhotsk and Japan. Of the nine regions, only the Bering Sea and the Gulf of St Lawrence show positive ice-extent trends on a yearly-average basis. However, the increases in these two regions are not statistically significant. For the north polar region as a whole, and for the Arctic Ocean, the Seas of Okhotsk and Japan, and Hudson Bay, the negative trends in the yearly averages are statistically significant at a 99% confidence level.

INTRODUCTION

Sea ice is an integral component of the Arctic climate system, restricting exchanges of heat, mass and momentum between the ocean and the atmosphere, reflecting most of the solar radiation incident upon it, releasing salt to the underlying ocean during freezing and transporting fresh water Equatorward through sea-ice advection. It is also of vital importance to the ecology of the Arctic, serving as a habitat for organisms living within it, a platform for animals wandering over it and either a help or a hindrance to numerous marine plant and animal species. Hence, changes in the sea-ice cover can have many outreaching effects on other elements of the polar climate and ecological systems. Furthermore, through the interconnectedness of the climate system, major changes in the sea-ice cover could have more far-reaching effects, extending well beyond the polar regions. For instance, changes in the ice transport of cold fresh water southward in the Greenland Sea could impact the deep-water formation in the northern North Atlantic and thereby affect the "conveyor-belt" circulation that cycles through much of the global ocean.

Considerable attention has been given recently to decreases in Arctic sea-ice extents detected through analysis of satellite passive-microwave data since late 1978 (e.g. Johannessen and others, 1995; Maslanik and others, 1996; Bjørgo and others, 1997; Parkinson and others, 1999). These studies have emphasized decreases examined for the record length as a whole or for annual or seasonal averages. Here we update the annual and seasonal decreases to a 21 year record through the end of 1999, and additionally present time series and trends for each month. Results are given for the Northern Hemisphere as a whole and for each of nine regions, identified in Figure 1. Although a much longer record would be desired (if available), this 21 year period does include El Niño and La Niña episodes, positive and negative phases of the North Atlantic Oscillation and the Arctic Oscillation, and major volcanic eruptions of El Chichón, Mexico (28 March–4 April 1982), and Mount Pinatubo, Philippines (15 June 1991). Hence it provides researchers studying those phenomena with a chance to examine effects they may have had on the Arctic sea-ice cover, thereby helping to quantify the respective climate interconnections.

DATA AND METHODOLOGY

The data used in this study are satellite passive-microwave data from the Nimbus 7 Scanning Multichannel Microwave Radiometer (SMMR) and three U.S. Defense Meteorological Satellite Program (DMSP) Special Sensor Microwave/Imagers (SSM/Is). Microwave data are particularly applicable for sea-ice research because the microwave emissions of sea ice and liquid water differ significantly, thereby allowing a ready distinction between ice and water from the satellite microwave data. Complications arise from the diversity of ice surfaces and from melt ponding and snow cover on the ice, but the satellite passive-microwave data still allow a clear depiction of the overall distribution of the ice and thereby allow a calculation of ice extents (areas covered by ice of concentration at least 15%).

The SMMR was operational on an every-other-day basis for most of the period 26 October 1978 to 20 August 1987, and the sequence of SSM/Is has been operational on a daily basis for most of the period since 9 July 1987. The SMMR and SSM/I data have been used to create a consistent dataset of sea-ice concentrations (per cent areal coverages of ice) and extents through procedures described in Cavalieri and others (1999). Briefly, the method used for obtaining consistency was one of matching sea-ice extents and areas during periods of overlap

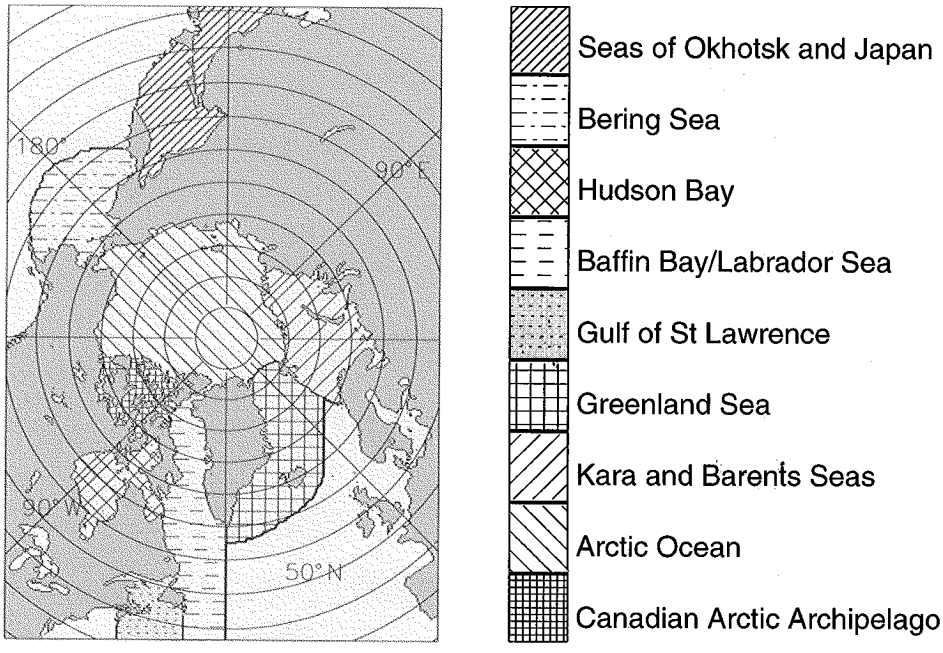

Fig. 1. Identification of the nine regions used in the analysis.

between consecutive sensors. This procedure reduced errors resulting from different sensor frequencies, footprint sizes, observation times and calibrations. While the periods of overlap were shorter than desirable, the average ice-extent differences between sensors were reduced to $<0.05\%$, and the average ice-area differences were reduced to 0.6% or less.

The ice concentrations are gridded to a resolution of approximately 25 km × 25 km (NSIDC, 1992) and are available at the U.S. National Snow and Ice Data Center (NSIDC) in Boulder, CO. The ice extents are calculated by adding the areas of all gridcells containing ice with a calculated concentration of at least 15%. This is done for each of the nine regions identified in Figure 1 and for the total.

Trends in the ice extents are determined through linear least-squares fits separately on the monthly-averaged, seasonally averaged and yearly-averaged data. The trends are calculated for each of the nine regions and the total, and in each case an estimated standard deviation of the trend (σ) is calculated following Taylor (1997). Trends are considered statistically significant in those cases where the trend magnitude exceeds 1.96σ, signifying a 95% confidence level that the slope is non-zero. Trends with magnitudes exceeding 2.58σ are considered significant at a 99% confidence level (Taylor, 1997).

DISCUSSION

Satellite technology provides a powerful resource for monitoring the Arctic sea-ice cover's distribution and extent, and we have taken advantage of this by using this technology to quantify changes in the Arctic ice cover since the late 1970s, with results presented in Table 1 and Figures 2–4 for the 21 year period 1979–99. Most notably, the ice cover as a whole has negative trends for every month, with a trend in the annual averages of $-32\,900 \pm 6100\ \mathrm{km^2\ a^{-1}}$.

Because of the sharp contrast between the microwave emissivities of liquid water and ice, the satellite passive-microwave data are particularly good at revealing the distribution of the sea-ice cover, which in turn allows calculation of the ice extent and determination of changes in ice extent. These satellite data are not as appropriate for determining changes in ice thickness, but analyses of submarine data have revealed a thinning of the ice cover (e.g. Rothrock and others, 1999) that is even more dramatic, percentage-wise, than the ice-extent reductions reported here. (However, Winsor (2001) reports that the thinning did not continue in the 1990s, at least over a limited region from north of Alaska to the North Pole.)

Of course neither the satellite data nor the submarine data can explain the causes of the sea-ice changes or predict future changes. If the decreasing ice coverage is tied most closely to an ongoing Arctic warming (Martin and others, 1997; Serreze and others, 2000) that continues, then the ice cover is likely to continue to decrease as well; but if the sea-ice changes are tied more closely to oscillatory behaviors in the climate system, such as the North Atlantic Oscillation and the Arctic Oscillation (as suggested by, e.g., Deser and others, 2000; Morison and others, 2000; Parkinson, 2000), then it is likely that there will also be fluctuations between periods of sea-ice decrease and periods of sea-ice increase.

Arctic Ocean

Claire L Parkinson
NASA Goddard Space Flight Center, Greenbelt, MD, USA

The Arctic Ocean is the smallest of the Earth's four major oceans (the Pacific, Atlantic, Indian, and Arctic), covering 14 $\times$ 10^6 km^2 located entirely within the Arctic Circle (66° 33′N). It is a major player in the climate of the north polar region, has a variable sea ice cover, and is home to a multitude of plant and animal species. Its temperature, salinity, and ice cover have all undergone changes in the past several decades, although it is uncertain whether these predominantly reflect long-term trends, oscillations within the system, or natural variability.

The Arctic Ocean is surrounded largely by the land masses of Eurasia, Greenland, and North America (Figure 1). Its principal connection to the rest of the Earth's oceans lies between Greenland and Scandinavia, where it connects to the North Atlantic. Smaller connections include the narrow (85 km wide) Bering Strait, linking it to the North Pacific, and the passageways within the Canadian Archipelago and between the Archipelago and Greenland, leading to Baffin Bay and thence to Davis Strait and the North Atlantic.

The Arctic Ocean has an unusually broad and shallow continental shelf on the Eurasian side, extending more than 1000 km northward from Scandinavia and approximately 800 km northward from Siberia. The deeper portion of the Arctic is divided by the Lomonosov Ridge into two main basins, the Canadian Basin and the smaller and deeper Eurasian Basin, which has a maximum depth exceeding 5000 m.

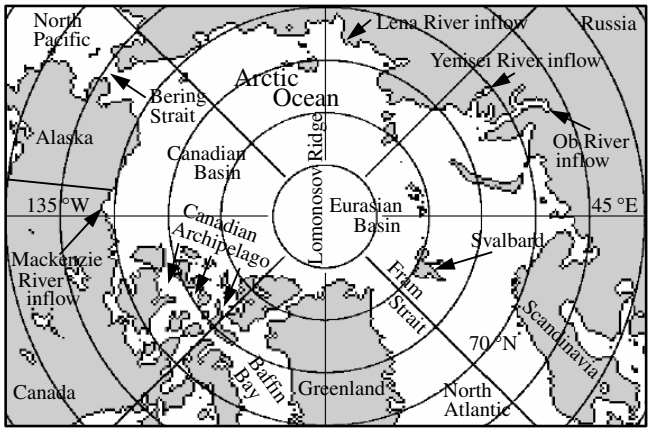

Figure 1 The Arctic Ocean and its surroundings

Water flows into the Arctic principally from the Atlantic as a warm, salty undercurrent. There are also smaller oceanic inputs through the Bering Strait and cold, freshwater inputs from many rivers, most significantly the Lena, Yenisei, and Ob rivers in Russia and the Mackenzie River in Canada. A large part of the outflow from the Arctic is through the Fram Strait between Greenland and Svalbard. Surface currents in the Arctic tend to be clockwise in the Canadian Basin, with occasional reversals to this flow, and more linear along the Transpolar Drift Stream flowing from north of Russia, across the Eurasian Basin and the vicinity of the North Pole, and out through Fram Strait (*see* **Ocean Circulation**, Volume 1).

The water inflows and outflows play a major role in the temperature and salinity structure of the Arctic (*see* **Salinity Patterns in the Ocean**, Volume 1). The warm, salty Atlantic layer from the Atlantic inflows is most prominent closest to the entrance regions but is also apparent throughout the Arctic at depths exceeding 200 m. Overlying the Atlantic layer, the Arctic surface water, in contact with the cold Arctic atmosphere and subject to the freshwater inputs from the surrounding rivers, is colder and less saline. The upper 30–50 m of the surface water tends to be fairly well mixed vertically, with temperatures near the freezing point and salinities ranging from highs exceeding 34 parts per thousand (ppt) near the North Atlantic to lows below 29 ppt near river inflows. Surface salinities in the Bering Strait are approximately 31 ppt. Vertically, salinities tend to increase with depth from the bottom of the mixed layer down to the Atlantic layer, with this vertical variation forming a prominent halocline, especially in the Eurasian Basin. The resulting stable density stratification hinders the warm Atlantic layer waters from upwelling to the surface.

Importantly, the Arctic Ocean is largely capped by a thin, broken layer of sea ice, generally less than 6 m thick and covered by snow (*see* **Sea Ice**, Volume 1). The sea ice restricts exchanges of heat, mass, and momentum between the ocean and the overlying atmosphere and, due to its high reflectivity, also tremendously restricts the input of solar radiation to the ocean. Ice covers almost all of the Arctic Ocean in winter, to an ice concentration (percent areal coverage) of at least 90%, and most of the Arctic Ocean in summer. Sea ice is considerably less saline than the ocean water from which it forms and tends to decrease in salinity over time, as more of the salt content is washed downward through the ice during periods of summer melt.

The Arctic ice cover is in constant flux, being melted by solar radiation, augmented by additional freezing, and moved by winds, waves, and currents. As ice floes separate, openings appear, called *leads* when linear and *polynyas* when large and non-linear. In contrast, when the forces acting on the ice result in floes colliding forcefully together,

the ice breaks and piles of ice rubble form. The above-water portions of these are called *ridges*, and the more massive underwater portions are called *keels*. A ridge/keel combination can have an ice thickness of 30 m or more, far exceeding the level-ice thickness.

Despite the cold temperatures, the Arctic is home to a host of plant and animal life, including algae colonizing the sea ice, sometimes at a concentration of millions in a single ice floe, and protozoans, crustaceans, and nematodes, most of which are smaller than 1 mm in length, also living in the ice and feasting upon the algae. Although biomass tends to be low under the permanent ice pack, high phytoplankton and zooplankton concentrations are frequently found in the ice-free waters. The resulting availability of food makes the ice-free waters popular for numerous species of birds and marine mammals. Amongst the larger animals, polar bears and Arctic foxes roam over the ice, and seals, walruses, and whales live in the ocean waters.

The Arctic has received considerable attention during the late 20th century and the start of the 21st century because of various changes reported to be occurring in it and the sense that these could be related to a possible global warming. Among the changes are the following:

1. A warming and spatial expansion of the Atlantic layer, at depths of 200–900 m, determined from ship-based conductivity–temperature–density (CTD) measurements in the 1990s versus data from 1950–1989 (Morison *et al.*, 2000; Serreze *et al.*, 2000).
2. A warming of the upper ocean in the Arctic's Beaufort Sea (north of Alaska) from 1975 to 1997, found from *in situ* measurements (McPhee *et al.*, 1998).
3. A considerable thinning, perhaps as high as 40%, of the Arctic sea ice cover in the second half of the 20th century, found from submarine data (Rothrock *et al.*, 1999).
4. A lesser and uneven retreat of the ice cover, averaging approximately 3% per decade between late 1978 and the end of 1996, found from satellite data (Bjørgo *et al.*, 1997; Parkinson *et al.*, 1999), and a related shortening of the length of the sea ice season throughout much of the region of the Arctic Ocean's seasonal sea ice cover, also found from satellite data (Parkinson, 2000).
5. An increase of 5.3 days per decade in the length of the melt season on the perennial ice cover, found from satellite data for 1979–1996 (Smith, 1998).
6. A decrease in the salinity of the upper 30 m of the central Beaufort Sea from 1975 to 1997, found from *in situ* measurements. This freshening of the water has been attributed largely to sea ice melt (McPhee *et al.*, 1998) and to increased runoff from the Mackenzie River (Macdonald *et al.*, 1999).
7. A mixed pattern of salinity increases and decreases through the expanse and depth of the rest of the Arctic Ocean (Morison *et al.*, 2000). This includes an increase in the salinity of the surface waters in the mid-Eurasian Basin during the 1990s, found from submarine data, and a thinning of the halocline separating the surface from the warm Atlantic layer waters (Steele and Boyd, 1998; Morison *et al.*, 2000).

In view of the highly coupled nature of the Arctic climate system, many of the changes occurring within it are likely connected. In particular, the freshening of the upper ocean in the Beaufort Sea is likely a response in part to the thinning of the ice, as ice melt adds freshwater to the upper ocean which consistently is much less saline than the ocean average. Similarly, the reduction in the sea ice cover and warming of the upper ocean are probably both connected to the Arctic surface air temperature increases reported, for instance, by Serreze *et al.* (2000).

The causes of the late-20th century changes in the Arctic system remain uncertain, although it is likely that several factors are involved. The increase in carbon dioxide and other greenhouse gases in the global atmosphere, is believed to cause atmospheric warming, although some human influences, such as the increase in particulate matter in the atmosphere, tend to offset a portion of the warming (*see* **Arctic Climate**, Volume 1). Atmospheric warming contributes to oceanic warming, sea ice melt, and upper ocean freshening, all observed in recent decades in portions of the Arctic.

Other potential influences, however, are more oscillatory in nature, such as the impacts of the North Atlantic Oscillation (NAO) and the Arctic Oscillation (AO), two major decadal-scale oscillations in atmospheric pressure patterns, or the impacts of El Niño/La Niña cycles. The NAO and AO in particular have received attention because many of the patterns of change in the ocean and ice cover of the Arctic can be explained by changes in the NAO and AO in recent decades (e.g., Parkinson *et al.*, 1999; Morison *et al.*, 2000). It remains uncertain, however, whether the changes in the NAO and AO are exclusively natural fluctuations in the climate system or are related to long-term, perhaps anthropogenically induced climate change (*see* **Arctic Oscillation**, Volume 1; **El Niño**, Volume 1; **North Atlantic Oscillation**, Volume 1).

Annals of Glaciology 34 2002

Trends in the length of the Southern Ocean sea-ice season, 1979–99

CLAIRE L. PARKINSON
Oceans and Ice Branch/Code 971, NASA Goddard Space Flight Center, Greenbelt, MD 20771, U.S.A.

ABSTRACT. Satellite passive-microwave data have been used to calculate and map the length of the sea-ice season throughout the Southern Ocean for each year 1979–99. Mapping the slopes of the lines of linear least-squares fit through the 21 years of resulting season-length data reveals a detailed pattern of trends in the length of the sea-ice season around the Antarctic continent. Specifically, most of the Ross Sea ice cover has, on average over the 21 years, undergone a lengthening of the sea-ice season, whereas most of the Amundsen Sea ice cover and almost the entire Bellingshausen Sea ice cover have undergone a shortening of the sea-ice season. Results for the Weddell Sea are mixed, with the northwestern portion of the sea having experienced a shortening of the sea-ice season but a substantial area in the south-central portion of the sea having experienced a lengthening of the ice season. Overall, the area of the Southern Ocean experiencing a lengthening of the sea-ice season by at least 1 day per year over the period 1979–99 is 5.6×10^6 km^2, whereas the area experiencing a shortening of the sea-ice season by at least 1 day per year is 46% less than that, at 3.0×10^6 km^2.

INTRODUCTION

The Southern Ocean (Fig. 1) sea-ice cover extends over a vast area, approximately 18×10^6 km^2, in the austral winter and experiences an enormous annual decay each spring and summer, with its coverage at the summer minimum typically reduced to $< 4 \times 10^6$ km^2 (Zwally and others, in press). The ice cover has a substantial impact on regional climate, most prominently by restricting exchanges of heat, mass and momentum between the ocean and the atmosphere and by reflecting most of the solar radiation incident on it. It also has a substantial impact on the biology of the Southern Ocean, for instance housing many species of micro-organisms, serving as a platform for penguins, seals and other animals, insulating marine life below the ice from the atmosphere, and reducing light penetration into the ocean. The reader is referred to Bentley (1984), Drewry and others (1993) and Worby and others (1996) for more on the climatological impacts of the ice and to Massom (1988), Drewry and others (1993) and Smith and others (1995) for more on the biological impacts of the ice, including the impacts on primary productivity, phytoplankton blooms, krill and breeding success in seabirds.

Until the 1970s, datasets regarding the Southern Ocean sea-ice cover tended to be sparse both temporally and spatially, due in large part to the vast area, the remoteness from most human habitations and the harshness of the in situ conditions. Fortunately, the ease of obtaining data on the ice cover changed dramatically with the advent of satellite technology. Satellite passive-microwave instrumentation in particular has allowed fairly routine monitoring of the Southern Ocean sea-ice cover since the late 1970s. In fact, the ease with which ice and water can be distinguished in passive-microwave data, due to the sharp contrast in ice and water emissivities at many microwave wavelengths, makes sea-ice coverage now amongst the most readily observed of all climate variables.

This paper takes advantage of satellite passive-microwave datasets over the 21 year period 1979–99 to report on changes in the length of the sea-ice season, defined as the number of days per year with sea-ice coverage, throughout the Southern Ocean. Changes in the length of the sea-ice season not only affect the regional climate and ecology, in ways alluded to above, but also can serve as indicators of change within the broader climate system. The length of

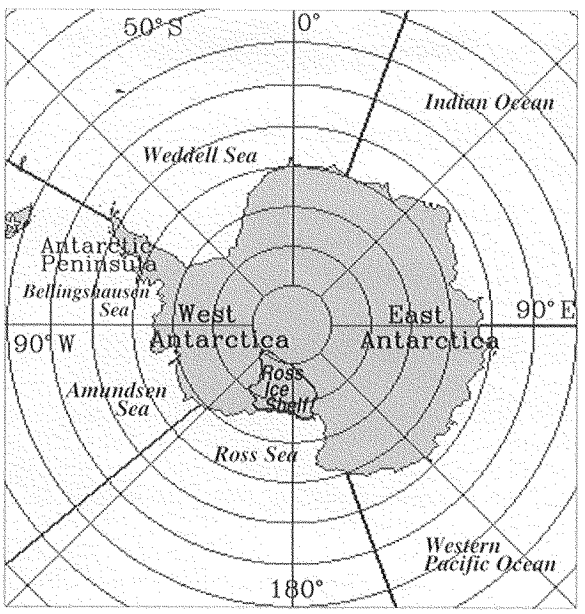

Fig. 1. Location map, including the boundaries of the five sectors into which the Southern Ocean is divided for analysis. The non-land boundaries are along the longitude lines at 20° E, 90° E, 160° E, 130° W and 60° W.

the sea-ice season was first examined and mapped for the Southern Ocean in Parkinson (1994), where results were presented for the 8 year period 1979–86. It has subsequently been examined for the 7 year period 1988–94 by Parkinson (1998) and for the two 8 year periods 1979–86 and 1989–96 by Watkins and Simmonds (2000).

DATA AND METHODOLOGY

This study uses data from the Nimbus 7 Scanning Multichannel Microwave Radiometer (SMMR) and the Defense Meteorological Satellite Program (DMSP) Special Sensor Microwave/Imagers (SSM/Is). The SMMR instrument collected data on an every-other-day basis for most of the period 26 October 1978 to 20 August 1987, and the SSM/Is have collected data on a daily basis for most of the period since 9 July 1987. The two datasets have been used by Cavalieri and others (1999) to create a consistent set of sea-ice concentrations (areal percentages of sea ice) using an algorithm commonly termed the NASA Team algorithm. This algorithm is based on the assumption of three surface types (two ice types plus liquid water), polarization and gradient ratios calculated from three channels of the satellite data, and a weather filter. The algorithm is described in detail in Gloersen and others (1992), and the procedures for matching the SMMR and SSM/I datasets are described in Cavalieri and others (1999). The ice concentrations have spatial resolutions of approximately 55 km and are gridded to a consistent grid with gridcell size approximately 25 × 25 km (NSIDC, 1992).

The sea-ice concentration data are used here to determine the length of the sea-ice season in each year at each gridpoint, by counting the number of days with ice coverage of at least 15%. Alternative ice-concentration cut-offs of 30% and 50% have also been used, with similar patterns resulting irrespective of which cut-off is selected (e.g. next section and Parkinson, 1994). The 15% cut-off is used for the main results in this paper both because it is the standard cut-off used for the ice-extent results from the same dataset (e.g. Zwally and others, in press) and because comparison of the ice concentrations from the NASA Team algorithm with those derived from other algorithms yields a close match in distributions of ice coverage of at least 15% but some substantial differences in distributions of ice of higher concentrations (e.g. Comiso and others, 1997; Hanna, 1999; Markus and Cavalieri, 2000). The 15% results are thus considered the most robust.

The trend in the length of the sea-ice season is calculated at each ocean gridpoint as the slope of the line of linear least-squares fit through the 21 years of season-length data. The calculations are done through matrix manipulations on the 21 annual matrices of the length of the sea-ice season for the 15% ice-concentration cut-off, and are then repeated for the 30% and 50% cut-offs. For the trend calculations, each year's season lengths are linearly scaled to equivalents for a 365 day year.

In order to obtain a measure of statistical significance for the trend results, an estimated standard deviation (σ) of the 21 year trend is calculated at each gridpoint following Taylor (1997). Trends are considered statistically significant when the trend magnitude exceeds 1.96σ, signifying a 95% confidence level that the slope is non-zero. Trends that additionally meet the criterion of exceeding 2.58σ are considered statistically significant at a 99% confidence level (Taylor, 1997).

SUMMARY AND DISCUSSION

Satellite passive-microwave data have been used to determine and map the length of the sea-ice season in each year 1979–99, with results showing (a) season lengths generally decreasing outward from the coast except in regions of coastal polynyas, (b) perennial ice cover consistently in the far-western Weddell Sea and more selectively elsewhere around the continent, and (c) decidedly short ice seasons (for the high latitudes involved) off the Ross Ice Shelf (Fig. 2). Trends in the season lengths over the 1979–99 period show that: (a) most of the Ross Sea underwent a lengthening of the sea-ice season, (b) most of the Amundsen Sea and almost the entire Bellingshausen Sea underwent a shortening of the sea-ice season, (c) the Weddell Sea had a shortening of the sea-ice season in the northwest but a lengthening of the season in a substantial area of the south-central sea, and (d) around much of East Antarctica, the near-coastal region experienced a lengthening of the season, while further from the coast there was a more even mixture of areas experiencing season shortenings and those experiencing season lengthenings (Fig. 3). Integrating spatially, a much larger area of the Southern Ocean experienced an overall lengthening of the sea-ice season over the 21 years 1979–99 than experienced a shortening (Fig. 4).

These results complement results on trends in the Southern Ocean ice extent (defined as the area having sea-ice concentrations of at least 15%) found from the SMMR and SSM/I record. Analyses of the regional and hemispheric ice extents for the 16 year period 1979–94 by Stammerjohn and Smith (1997) and for the 20.2 year period from November 1978 through December 1998 by Zwally and others (in press) reveal positive ice-extent trends for the Weddell Sea, the Western Pacific Ocean, the Ross Sea and the Southern Ocean as a whole and negative ice-extent trends for the Bellingshausen and Amundsen Seas. The mapped results of the trends in the length of the sea-ice season (Fig. 3) provide a far more detailed spatial picture of the 21 year changes in the Southern Ocean than is possible when examining the ice extents, but at the same time, they provide a far less detailed temporal picture. Together, the ice-extent and season-length results show an overall increasing Southern Ocean ice cover, with the Bellingshausen and Amundsen Seas and the far-western and northwestern Weddell Sea showing instead ice-cover decreases. These results are consistent with reports of notable warming over the Antarctic Peninsula from 1978 to 1996 (King and Harangozo, 1998; Skvarca and others, 1998; both studies also include years prior to 1978) and with a tendency for air-temperature anomalies in the peninsula region to be opposite in sign to those predominating over much of the rest of the Antarctic (Rogers, 1983; Stammerjohn and Smith, 1997).

The satellite-derived Southern Ocean sea-ice results, with overall lengthening sea-ice seasons (Figs 3 and 4) and increasing ice extents (Stammerjohn and Smith, 1997; Zwally and others, in press), provide a sharp contrast with the widely publicized overall ice-cover decreases in the Arctic occurring over the same period. Many uncertainties remain, but one certainty is that the ice covers of the two hemispheres have not been fluctuating synchronously over the past two decades.

Annals of Glaciology 34 2002

In situ and satellite surface temperature records in Antarctica

CHRISTOPHER A. SHUMAN,[1,2] JOSEFINO C. COMISO[2]
[1]*Earth System Science Interdisciplinary Center, University of Maryland, College Park, MD 20742-2465, U.S.A.*
[2]*Oceans and Ice Branch, Laboratory for Hydrospheric Processes, NASA Goddard Space Flight Center, Code 971, Greenbelt, MD 20771, U.S.A.*

ABSTRACT. Air-temperature records (T_A) during 1992 from five inland Antarctic automatic weather station (AWS) sites were compared with the best available infrared temperatures (T_{IR}) from the Advanced Very High Resolution Radiometer (AVHRR) as well as calibrated passive-microwave temperatures (T_C) from the Special Sensor Microwave/Imager (SSM/I). Daily and monthly average T_A, T_{IR}, and T_C data indicate that each approach captures generally similar trends at each site but each approach also has limitations. AWS T_A data are considered the most accurate but represent spatially restricted areas and may have long gaps due to sensor or transmission problems. AVHRR T_{IR} data have daily variability similar to the T_A record but have numerous small gaps due to cloud cover or observation interruptions. An offset between T_A and T_{IR} (>4 K) at the South Pole site was identified that may be due to the inclusion of data with large satellite scan angles necessary to cover this area. SSM/I T_C data have the most continuity but exhibit calibration problems, a significantly damped daily response and do not cover all of Antarctica. Individual daily differences between T_A and T_{IR} as well as T_A and T_C can exceed 17 K, but all sites have mean daily differences of about 1 K or better, after compensating for the offset at South Pole, and standard deviations of <6 K. Monthly temperature differences are typically 5 K or better, with standard deviations generally <3 K. And finally, using the available data, the 1992 average temperature differences are <1 K.

INTRODUCTION

Detection of climate change involves determining a multi-year baseline for a climate parameter and then detecting variations that exceed its observed range over the baseline period. Increasing temperatures, possibly linked to global climate warming, have been detected at sites on the Antarctic Peninsula (Jacka and Budd, 1991; King, 1994; Vaughan and Doake, 1996). Further inland, at specific automatic weather stations (AWSs), data on near-surface temperature (T_A) are beginning to define a climate baseline (Shuman and Stearns, 2001). However, these data have significant gaps and may not be representative of broader regional or continental-scale patterns. Temperature fields derived from satellite infrared (Comiso, 2000) or passive-microwave sensors can provide a much more complete characterization of spatial and temporal variations in Antarctic temperature. Currently, the only spatially detailed record of surface temperature across Antarctica is provided by Advanced Very High Resolution Radiometer (AVHRR) infrared channels (T_{IR}), but they must be carefully processed to remove the effects of clouds (Comiso, 2000). Passive-microwave data from the 37 GHz channel of the Special Sensor Microwave/Imager (SSM/I) are not influenced by cloud cover and can be calibrated (T_C) at specific AWS locations (Shuman and others, 1995) or by complex radiative transfer models (Fung and Chen, 1981; Comiso and others, 1982), but cannot yet be broadly extrapolated in space and time because of still poorly understood spatial variations in the emissivity of the surface. Time series of these satellite data, if they could be used consistently, would provide the temperature data needed to identify regional and continental-scale climate change across Antarctica. This study, using recently published temperature data, analyzes in situ and satellite temperature information, and documents the advantages and limitations of each approach. The intent of this study is to use the AWS data to gain insight into the accuracy of the surface temperatures retrieved from satellite infrared and microwave sources and establish confidence limits on these data.

Table 1. Site data for inland Antarctic AWS temperature records

AWS name	*Location*	*Elevation*	*Grid*	*Start*	*Stop*
		m			
Byrd	80.01° S, 119.40° W	1530	121 196	Feb. 1980	
Clean Air	90.00° S, 120.00° W	2835		Jan. 1986	
Lettau	82.52° S, 174.45° W	55	155 206	Jan. 1986	
Lynn	74.21° S, 160.41° E	1772	182 239	Jan. 1988	Jan. 1998
Siple	75.90° S, 84.00° W	1054	97 168	Jan. 1982	Apr. 1992

Notes: This analysis is based on available 3 hourly average data taken from the University of Wisconsin server in March 1999. The grid column contains the coordinates of the 25 km SSM/I pixel covering the AWS location. There is no SSM/I coverage at the South Pole, where AWS Clean Air is located.

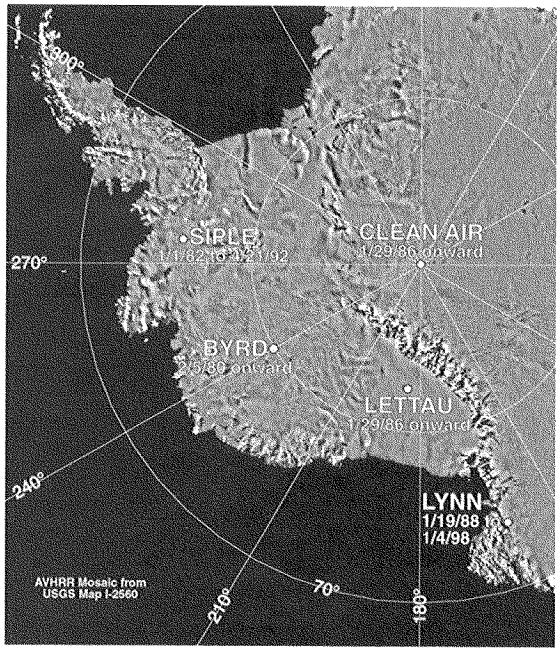

Fig. 1. The locations and dates of operation of the five inland Antarctic AWSs used in this study. Dates are mm/dd/yy.

This project used three types of temperature data from 1992 that were spatially and temporally co-registered:

(1) daily-average T_A records from five AWSs in Antarctica operated by the University of Wisconsin (see Fig. 1; Table 1);

(2) daily-average AVHRR T_{IR} data compiled and processed as described in Comiso (2000); and

(3) daily-average T_C data derived from the SSM/I datasets compiled by the U.S. National Snow and Ice Data Center (NSIDC) and calibrated as described in Shuman and Stearns (2001).

The three measurements are not exactly for the same physical parameter since the AWS measures near-surface air temperature (~2 m), the infrared sensor measures skin-depth temperature, and the passive-microwave sensor measures the average temperature of the upper surface layer. This comparative analysis will help establish how the three datasets can be used in conjunction to study the variations of an important climate parameter through time.

CONCLUSIONS

The significance of this study is that it enabled an improved understanding of three currently available Antarctic surface temperature datasets. At present, the thermal infrared data provide the only spatially detailed temperature distributions in Antarctica, but contain data gaps due to intermittent cloud cover. The passive-microwave data have the potential to provide spatially detailed, continuous and gap-free temperature distributions. However, more research is needed to correctly calibrate these data for regional changes in the radiative characteristics of the snow cover. The AWS data are the most accurate, but are the most difficult to use for large-scale scientific research because of their limited spatial coverage and gaps in the temporal series due to occasional instrument malfunction. The AWS data, however, provide the means to determine the value and the significance of both the infrared and the passive-microwave datasets.

Table 4. Difference statistics for all 1992 T_{IR} and T_C daily mean temperatures

	Byrd	*Clean Air*	*Lettau*	*Lynn*	*Siple*
Days	323	305	313	342	328
T_{IR}	245.66	226.38	246.97	238.85	248.12
T_C	247.02		246.64	237.64	247.61
$T_{IR} - T_C$	−1.36		0.33	1.21	0.52

Notes: This analysis is based on all days where there was both an AVHRR infrared temperature (T_{IR}) and a calibrated SSM/I temperature (T_C). There are no T_C data for AWS Clean Air due to the hole in SSM/I coverage at the South Pole.

These different near-surface temperature datasets are quite complementary and should enable the development of improved temperature baselines for sites in Antarctica. Although T_A data may be discontinuous, T_{IR} data can accurately fill most gaps at specific sites. Any gaps due to cloud cover in the T_{IR} record can then be filled with extrapolated T_C values, and these values also provide a reliability check on the spatially more extensive T_{IR} data. Processing requirements are significant, especially for T_{IR}, however, and detecting and removing cloud impacts and accurately calibrating these data remains a challenge. Overall, this study has demonstrated that the satellite data compare quite well in most cases, assuming that these AWS T_A data reliably represent these locations. The limited comparisons presented here certainly justify continued efforts with additional years of data at these and other sites across the Antarctic continent. Although individual day differences between in situ and satellite temperatures can be quite large, the average errors are relatively small and appear well constrained. For the thermal infrared dataset, the standard products are the monthly averages that appear to provide a realistic representation of temperature distributions around the continent. Some of the discrepancies between the methods studied here are probably due to the differing spatial and temporal resolutions of the three different methods. We also have assumed that the AWS hardware for measuring temperature is always in perfect condition, which is not guaranteed in such an adverse environment, and there may be some instances when the AWS actually provides erroneous results despite quality-control procedures. For optimal accuracy, especially at high temporal resolution, a combination of the three methods may be necessary to determine an accurate climate baseline and then evaluate potential changes that may come in the years ahead.

Analysis of seasonal cycles in climatic trends with application to satellite observations of sea ice extent

Konstantin Y. Vinnikov
Department of Meteorology, University of Maryland, College Park, Maryland, USA

Alan Robock
Department of Environmental Sciences, Rutgers University, New Brunswick, New Jersey, USA

Donald J. Cavalieri and Claire L. Parkinson
Oceans and Ice Branch, NASA Goddard Space Flight Center, Greenbelt, Maryland, USA

Received 29 November 2001; accepted 8 January 2002; published 8 May 2002.

[1] We present a new technique to study the seasonal cycle of climatic trends in the expected value, variance, and other moments of the statistical distribution. The basis of the technique is multiple linear regression, but with periodic basis functions. The technique allows us to provide comprehensive information on statistical parameters of climate for every day of an observational period. Using daily data, the technique has no problems caused by different lengths of months or the leap-year cycle. Without needing to assume the stationarity of contemporary climate, the technique allows the study of statistical parameters of climatic records of arbitrary length. We illustrate the technique with applications to trends in the satellite observed variations of sea ice extent in the Northern and Southern Hemispheres. We show that a significant part of the variability in hemispheric sea ice extents for the period 1978–1999 is related to linear trends. *INDEX TERMS:* 1620 Global Change: Climate dynamics (3309); 1866 Hydrology: Soil moisture; 3309 Meteorology and Atmospheric Dynamics: Climatology (1620); 4215 Oceanography: General: Climate and interannual variability (3309)

1. Introduction

[2] Traditional climatology uses monthly averages and statistics estimated for 30-yr time intervals. This approach, however, has well-known limitations. Monthly averages incorporate different lengths for different months and different years (leap years). Using only 12 monthly averages is a very crude approximation of the seasonal variation for many meteorological variables and produces biases in the spectrum of meteorological records. Time series for specific months are too short to estimate the parameters of the statistical distribution of monthly averages properly.

[3] Here we introduce a new statistical approach to analyzing climate data that explicitly accepts the idea that long-term climatic records may contain trends in means, variances, covariances, and other moments of the statistical distribution of meteorological variables. We also explicitly permit seasonal cycles of these trends. This approach is designed to analyze observed past climate change and climate model output, but is not designed to be used to extrapolate the trends into the future.

2. Theory

[4] We start by using daily observations instead of monthly averages. Let us denote

$$y(t) = Y(t) + y'(t); \tag{1}$$

where $y(t)$ is the observed value of y for day number t, $t = t_1, t_2, t_3, \ldots, t_n$; $Y(t)$ is the expected value of $y(t)$; and $y'(t)$ is the residual (anomaly). We can use as t the Julian day number, or choose any other specific date as the reference day ($t = 0$).

[5] A common approach in studies of the seasonal cycle is to use Fourier harmonics of the annual period to approximate the seasonal variation of the mean values of the observed data [*Anderson*, 1971; *Polyak*, 1975]. It is well known that climatic trends may be different for different seasons [*Mitchell*, 1961; *Vinnikov*, 1986; *Hansen and Lebedeff*, 1987; *Chapman and Walsh*, 1993; *Stammerjohn and Smith*, 1997; *Hansen et al.*, 1999; *Parkinson et al.*, 1999; *Jones et al.*, 1999; *Rigor et al.*, 2000; *Serreze et al.*, 2000]. Let us assume that the climatic trend in the expectation $Y(t)$ of the observed variable $y(t)$ is a periodic function of the annual period. Particularly, for a linear trend this means:

$$Y(t) = A(t) + B(t) \cdot t, \tag{2}$$

where $A(t) = A(t + T)$, $B(t) = B(t + T)$, and $T = 365.25$ days. Let us use a limited number of Fourier harmonics to approximate both periodic functions, $A(t)$ and $B(t)$:

$$Y(t) = a_0 + \sum_{k=1}^{K}\left[a_k \sin\left(\frac{2\pi kt}{T}\right) + b_k \cos\left(\frac{2\pi kt}{T}\right)\right] + \alpha_0 t + \sum_{m=1}^{M}\left[\alpha_m t \sin\left(\frac{2\pi mt}{T}\right) + \beta_m t \cos\left(\frac{2\pi mt}{T}\right)\right]. \tag{3}$$

We can estimate all the unknown multiple regression coefficients in (3) from the least squares condition:

$$\sum_{t=t_1}^{t_n}[y(t) - Y(t)]^2 = F(a_0, \ldots, a_K, b_1, \ldots, b_K, \alpha_0, \ldots, \alpha_M, \beta_1, \ldots, \beta_M) = \min. \tag{4}$$

The number of harmonics required for approximation of $A(t)$ and $B(t)$, K, and M, should be chosen from independent considerations or should be estimated from analyses of the same data.

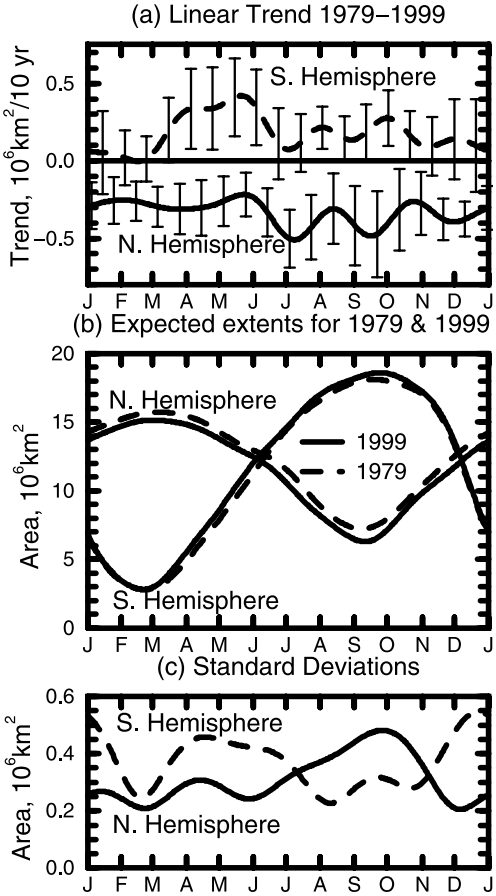

Figure 3. Sea ice extents in the Northern and Southern Hemispheres: (a) linear trend 1979–1999, (b) expected extent for years 1979 and 1999, (c) standard deviations of daily extents, 1979–1999.

4. Discussion and Conclusions

[10] Most previous analyses of trends in sea ice extents have produced statistics for monthly or yearly averages. Daily observations give us an opportunity to see additional interesting details in the same climatic records. Results of applying the new technique to sea ice extents yield the following conclusions:

4.1. Northern Hemisphere Sea Ice Extent

[11] The expected sea ice extent in the Northern Hemisphere has been decreasing during 1979–1999 for each day of the year with rates from -0.2×10^6 km^2/10 yr to -0.5×10^6 km^2/10 yr (Figures 3a and 3b). Consistently, although in less detail, *Parkinson and Cavalieri* [2002] find that monthly trends in the Northern Hemisphere ice extents have negative values for all 12 months, all with magnitudes of at least -0.23×10^6 km^2/10 yr.

[12] The expected maximum seasonal sea ice extent in 1999 was about 0.5×10^6 km^2 less than it was in 1979 (Figure 1, line (a)). This corresponds to a $\sim$0.3° latitude poleward shift of the average position of the sea ice boundary at the time of its maximum seasonal expansion.

[13] The expected minimum seasonal sea ice extent in 1999 was about 1.0×10^6 km^2 less than it was in 1979 (Figure 1, line (b)). This corresponds to a $\sim$1° latitude poleward shift of the average position of the sea ice boundary at the time of its maximum seasonal retreat.

[14] The average amplitude of the seasonal variation in sea ice extent has increased about 0.5×10^6 km^2 during the 21-year period 1979–1999, from $\sim 8.5 \times 10^6$ km^2 to $\sim 9.0 \times 10^6$ km^2 (Figure 1).

[15] Daily anomalies of sea ice extent (Figure 1) are an order of magnitude smaller than the seasonal variation of sea ice extent (about $8.5–9.0 \times 10^6$ km^2/10 yr, Figure 1).

[16] Trend-related changes during the last two decades of the 20th Century have the same order of magnitude ($0–1 \times 10^6$ km^2) as daily anomalies of sea ice extent (Figure 1).

4.2. Southern Hemisphere Sea Ice Extent

[17] The expected sea ice extent in the Southern Hemisphere has been increasing during 1979–1999 for almost every day of the year, with rates up to $\sim 0.4 \times 10^6$ km^2/10 yr (Figures 3a and 3b). This asymmetry between Northern and Southern Hemisphere sea ice variation was predicted using a climate model forced by increasing greenhouse gases [*Manabe et al.*, 1992] and then observed through satellite microwave measurements [*Cavalieri et al.*, 1997].

[18] The expected seasonally maximum sea ice extent in 1999 is about 0.5×10^6 km^2 larger than it was in 1979 (Figure 2, line (a)). There is no noticeable trend in sea ice extent at the time of its maximum seasonal retreat (Figure 2, line (b)). The average amplitude of seasonal variation in sea ice extent has increased about 0.5×10^6 km^2 during the 21-year period, from $\sim 15.3 \times 10^6$ km^2 to $\sim 15.8 \times 10^6$ km^2. Thus the seasonal amplitude of sea ice extent has increased in both hemispheres, and in both cases by about 0.5×10^6 km^2 (Figures 1 and 2).

[19] Daily anomalies of sea ice extent in the Southern Hemisphere (Figure 2) are an order of magnitude smaller than the seasonal variation of sea ice extent (Figure 3b), the same as in the Northern Hemisphere.

[20] As in the Northern Hemisphere, daily anomalies in the Southern Hemisphere are generally between -1×10^6 km^2 and 1×10^6 km^2 (Figures 1 and 2), although the 1979–1999 trends are generally smaller in magnitude, as well as being opposite in sign (Figure 3a).

4.3. Further Development of the Technique

[21] Harmonic functions may not be optimal for approximation of seasonal variations of many climatic variables. Other classes of periodic functions may be used, and empirical statistically orthogonal functions should be considered as possible alternatives to harmonic functions.

[22] In some cases, significant seasonal variations can exist in the variance of climatic indices. In such cases, it might be useful to repeat the calculations using a "weighted least squares" with weights that are inversely proportional to the estimated variance.

[23] Trend estimates for each day of a year provide information about the seasonality of trends in moments of the statistical distribution of climatic variables. The same technique can be applied to analyze time series of observed climatic indices at every specific time of a day. In the case when we have hourly meteorological observations, we can put together the estimates for every hour and receive a full picture of seasonal and diurnal cycles in climatic trends. Joint analysis of the seasonal and diurnal cycles in climatic trends will be discussed in another paper.

[24] The existing traditional practice of climatic services is based on monthly averages and a 30-year period for normals. Even for a variable with an autocorrelation time scale of 50 days, such as sea ice, this technique provides high temporal resolution depictions of the seasonal cycles of the means, anomalies, and trends (Figures 1–3). Without needing to assume the stationarity of contemporary climate, our approach allows the study of statistical parameters of climatic records of arbitrary length. This opens a new opportunity to modernize existing climate services.

Variability of Antarctic sea ice 1979–1998

H. Jay Zwally, Josefino C. Comiso, Claire L. Parkinson, Donald J. Cavalieri, and Per Gloersen

Oceans and Ice Branch, NASA Goddard Space Flight Center, Greenbelt, Maryland, USA

Received 22 November 2000; revised 23 July 2001; accepted 13 September 2001; published 16 May 2002.

[1] The principal characteristics of the variability of Antarctic sea ice cover as previously described from satellite passive microwave observations are also evident in a systematically calibrated and analyzed data set for 20.2 years (1979–1998). The total Antarctic sea ice extent (concentration >15%) increased by 11,180 ± 4190 km^2 yr^{-1} (0.98 ± 0.37% (decade)$^{-1}$). The increase in the area of sea ice within the extent boundary is similar (10,860 ± 3720 km^2 yr^{-1} and 1.26 ± 0.43% (decade)$^{-1}$). Regionally, the trends in extent are positive in the Weddel Sea (1.4 ± 0.9% (decade)$^{-1}$), Pacific Ocean (2.0 ± 1.4% (decade)$^{-1}$), and Ross (6.7 ± 1.1% (decade)$^{-1}$) sectors, slightly negative in the Indian Ocean (−1.0 ± 1.0% (decade)$^{-1}$), and strongly negative in the Bellingshausen-Amundsen Seas sector (−9.7 ± 1.5% (decade)$^{-1}$). For the entire ice pack, ice increases occur in all seasons, with the largest increase during fall. On a regional basis the trends differ season to season. During summer and fall the trends are positive or near zero in all sectors except the Bellingshausen-Amundsen Seas sector. During winter and spring the trends are negative or near zero in all sectors except the Ross Sea, which has positive trends in all seasons. Components of interannual variability with periods of about 3–5 years are regionally large but tend to counterbalance each other in the total ice pack. The interannual variability of the annual mean sea ice extent is only 1.6% overall, compared to 6–9% in each of five regional sectors. Analysis of the relation between regional sea ice extents and spatially averaged surface temperatures over the ice pack gives an overall sensitivity between winter ice cover and temperature of −0.7% change in sea ice extent per degree Kelvin. For summer some regional ice extents vary positively with temperature, and others vary negatively. The observed increase in Antarctic sea ice cover is counter to the observed decreases in the Arctic. It is also qualitatively consistent with the counterintuitive prediction of a global atmospheric-ocean model of increasing sea ice around Antarctica with climate warming due to the stabilizing effects of increased snowfall on the Southern Ocean. *INDEX TERMS:* 1620 Global Change: Climate dynamics (3309); 1635 Global Change: Oceans (4203); 1640 Global Change: Remote sensing; 4207 Oceanography: General: Arctic and Antarctic oceanography; *KEYWORDS:* sea ice, Antarctic, climate, passive microwave, Southern Ocean

1. Introduction

[2] In recent decades the Antarctic sea ice cover has varied significantly from year to year with some anomalies persisting for periods of 3–5 years [e.g., *Zwally et al.*, 1983a]. However, decadal-scale sea ice changes have been smaller and more difficult to ascertain with statistical significance. Furthermore, while the physical processes (ice-ocean-atmosphere-solar) that control the annual growth and decay of sea ice are well known, the manner in which these processes combine on decadal timescales and regional spatial scales is complex and not well determined. In particular, the interaction of the Antarctic sea ice cover with global climate change is uncertain. In one view the intuitive expectation that a smaller sea ice cover should be associated with warmer atmospheric temperatures is supported by some observations and models. For example, *Gordon and O'Farrell* [1997] modeled a decreasing Antarctic sea ice cover in a warmer climate but with a smaller rate of decrease than their modeled rate of decrease for the Arctic sea ice. Observationally, *Jacka and Budd* [1991] and *Weatherly et al.* [1991] also showed the expected negative correlation between regional-scale sea ice changes and Antarctic coastal air temperatures. In another view, at least one climate model, which included coupled ice-ocean-atmosphere interactions [*Manabe et al.*, 1992], gives the counterintuitive result that the sea ice cover would actually increase with global climate warming. The physical processes in the model that cause the predicted sea ice increase are increased precipitation with a warmer atmosphere in polar regions, more snowfall on sea ice, lower salinity in the near-surface ocean layers, more stable mixed layer and reduced heat flux to the surface, and consequently, more sea ice.

[3] Clearly, if changes in the distribution of Antarctic sea ice are expected to be indicative of global climate change, a better understanding of the nature and causes of Antarctic sea ice variability is required. In particular, we should know whether Antarctic sea ice is expected to increase or decrease with climate warming. In this paper we describe the variability of the Antarctic ice cover in detail, including the variations in regional sectors as defined by *Zwally et al.* [1983b] and *Gloersen et al.* [1992], using 20 years of well-calibrated data. We believe the characteristics of the observed sea ice variability of the Antarctic provide new insights to the interplay of the relevant physical and climatic processes on seasonal to decadal timescales. In particular, our analysis of the decadal-scale trends in sea ice by season show that the trend of increasing Antarctic sea ice cover is dominated by summer and autumn increases and that changes in the winter are near zero overall. These results are important because the dominant climatic processes controlling the distribution of sea ice around the time of the winter maximum extent are likely to be

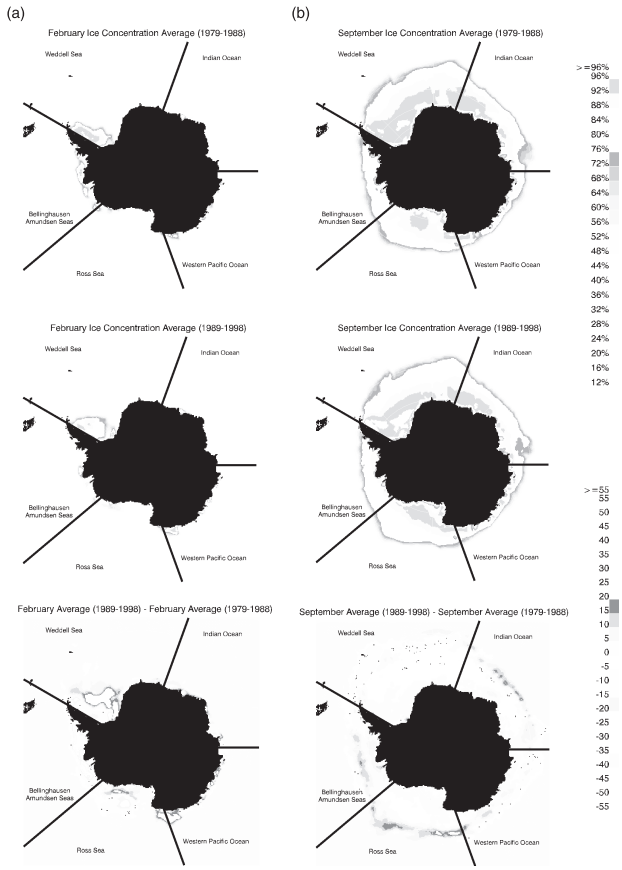

Figure 1. Average sea ice concentration maps averaged over (top) the first 10 years (1979–1988) and (middle) the second 10 years (1989–1998) and (bottom) their differences for (a) February, the month of summer minimum and (b) September, the month of winter maximum. The five regional sectors are Weddell Sea (60°W–20°E), Indian Ocean (20°–90°E), Pacific Ocean (90°–160°E), Ross Sea (160°–140°W), and Bellingshausen-Amundsen Seas (140°–60°W). See color version of this figure at back of this issue.

significantly different than those near the summer minimum. Examination of potential correlations between temperature (using new satellite estimates of surface temperature averaged over the sea ice pack) and sea ice extent shows a wintertime correlation on a regional basis, which gives an estimate of the sensitivity of sea ice cover to temperature change.

2. Background

[4] Since the advent of satellite remote sensing, the study of interannual changes in the Antarctic sea ice cover and their possible climatic significance have been the subject of numerous investigations. Initially, the use of relatively short or poorly calibrated satellite historical records caused some conflicting results regarding trends in ice extent [e.g., *Kukla*, 1978; *Kukla and Gavin*, 1981; *Zwally et al.*, 1983a]. Even with the sole use of longer and more consistent passive microwave data, the trends from analysis of the same set of satellite data have differed [*Johannessen et al.*, 1995; *Bjørgo et al.*, 1997; *Cavalieri et al.*, 1997; *Stammerjohn and Smith*, 1997]. This is partly because the satellite sensors have finite lifetimes and the time series is made up of measurements from different sensors, some of which have different footprints and characteristics than the others. Furthermore, different investigators use different ice algorithms for the retrieval of ice parameters and their own techniques for removing abnormal values in the land/ocean boundaries and the open ocean. During periods of overlap the different sensors also provide slightly different sea ice extents and actual areas, even with the same techniques. Therefore further intersensor adjustments are required to match the overlap results and obtain a uniform time series.

[5] For the period of November 1978 through December 1996, *Cavalieri et al.* [1997] found an asymmetry in the trends of decreasing Arctic sea ice extent ($-2.9 \pm 0.4\%$ (decade)$^{-1}$) and increasing Antarctic sea ice extent ($+1.3 \pm 0.2\%$ (decade)$^{-1}$). *Cavalieri et al.* [1997] also reviewed the results of previous analyses, which used essentially the same multisatellite passive microwave data set but with some different methodologies and conclusions about the apparent trends in the Antarctic sea ice. The methodologies for sea ice mapping and intersatellite calibration techniques employed by *Cavalieri et al.* [1997] to produce a data [e.g., see *Steffen et al.*, 1992].

9. Discussion and Conclusions

[51] A primary result of this analysis of the 20 years of measurements of sea ice concentration on the Southern Ocean is the $+11{,}181 \pm 4190$ km^2 yr^{-1} ($+0.98 \pm 0.37\%$ (decade)$^{-1}$) increase in sea ice extent and a very similar $+10{,}860 \pm 3720$ km^2 yr^{-1} ($+1.26 \pm 0.43\%$ (decade)$^{-1}$) increase in sea ice area. Regionally, the trends in extent are positive in the Weddell Sea ($1.4 \pm 0.9\%$ (decade)$^{-1}$), Pacific Ocean ($2.0 \pm 1.4\%$ (decade)$^{-1}$), and Ross Sea ($6.7 \pm 1.1\%$ (decade)$^{-1}$) sectors, slightly negative in the Indian Ocean ($-1.0 \pm 1.0\%$ (decade)$^{-1}$), and negative in the Bellingshausen/Amundsen Seas sector ($-9.7 \pm 1.5\%$ (decade)$^{-1}$). An overall increase in Antarctic sea ice cover, during a period when global climate appears to have been warming by 0.2 K (decade)$^{-1}$ [*Hansen et al.*, 1999], stands in marked contrast to the observed decrease in the Arctic sea ice extent of $-34{,}300 \pm 3700$ km^2 yr^{-1} ($-2.8 \pm 0.3\%$ (decade)$^{-1}$) and sea ice area of $-29{,}500 \pm 3800$ km^2 yr^{-1} ($-2.8 \pm 0.4\%$ (decade)$^{-1}$) in sea ice area [*Parkinson et al.*, 1999]. The observed decrease in the Arctic has been partially attributed to greenhouse warming through climate model simulations with increased CO_2 and aerosols [*Vinnikov et al.*, 1999]. As discussed in section 1, an increasing Antarctic sea ice cover is consistent with at least one climate model that includes coupled ice-ocean-atmosphere interactions and a doubling of CO_2 content over 80 years [*Manabe et al.*, 1992].

[52] Another main aspect of the results is the seasonality of the changes, being largest in autumn in both magnitude ($+24{,}700 \pm 17{,}500$ km^2 yr^{-1}) and percentage ($+2.5 \pm 1.8\%$ (decade)$^{-1}$) and second largest in summer ($+6700 \pm 12{,}600$ km^2 yr^{-1} and $+1.7 \pm 3.2\%$ (decade)$^{-1}$) in terms of percentage change. The changes for the winter season ($+7400 \pm 8500$ km^2 yr^{-1} and $+0.4 \pm 0.5\%$ (decade)$^{-1}$) and for spring ($+10{,}100 \pm 14{,}000$ km^2 yr^{-1} and $+0.7 \pm 1.0\%$ (decade)$^{-1}$) are small as a fractional change. On a regional basis the trends differ season to season. During summer and fall the trends are positive or near zero in all sectors except the Bellingshausen/Amundsen Seas sector. During winter and spring the trends are negative or near zero in all sectors except the Ross Sea, which has positive trends in all seasons.

[53] In the context of climate change the sensitivity of the sea ice to changes in temperature is of particular interest. Analysis of the relation between regional sea ice extents and spatially averaged surface temperatures over the ice pack gives an overall sensitivity between winter ice cover and temperature of -0.70% change in sea ice extent per degree Kelvin ($-0.11 \pm 0.09 \times 10^6$ km^2 K^{-1}). A change in the winter ice extent of 0.70% corresponds to a latitudinal change in the average position of ice edge of <10 km or a meridional change of <0.1°, which is small compared to some previous estimates [e.g., *Parkinson and Bindschadler*, 1984]. For summer some regional ice extents vary positively with temperature, and others vary negatively.